Delivery of loaded MR1 monomer results in efficient ligand exchange to host MR1 and subsequent MR1T cell activation

Corinna A. Kulicke[1,#], Gwendolyn M. Swarbrick[2,#], Nicole A. Ladd[3], Meghan Cansler[2], Megan Null[2], Aneta Worley[1], Chance Lemon[1], Tania Ahmed[2], Joshua Bennett[2], Taylor N. Lust[1], Chelsea M. Heisler[1], Megan E. Huber[5], Jason R. Krawic[6], Laurisa M. Ankley[7], Savannah K. McBride[5], Fikadu G. Tafesse[5], Andrew J. Olive[7], William H. Hildebrand[6], Deborah A. Lewinsohn[2], Erin J. Adams[3], David M. Lewinsohn[1,4, &], Melanie J. Harriff*[1,4, 5, &]

Affiliations

[1]Division of Pulmonary, Allergy, and Critical Care Medicine, Oregon Health & Science University, Portland, OR 97239, USA

[2]Division of Infectious Diseases, Department of Pediatrics, Oregon Health & Science University, Portland, OR 97239, USA

[3]Department of Biochemistry and Molecular Biology, University of Chicago, Chicago, IL 60637, USA

[4]VA Portland Health Care System, Portland, OR 97239, USA

[5]Department of Molecular Microbiology and Immunology, Oregon Health & Science University, Portland, OR 97239, USA

[6]Department of Microbiology and Immunology, University of Oklahoma Health Sciences Center, Oklahoma City, OK 73104, USA

[7]Department of Microbiology and Molecular Genetics, College of Osteopathic Medicine, Michigan State University, East Lansing, MI 48824 , USA

[#] These authors contributed equally

[&] These authors jointly supervised this work

* corresponding author: harriffm@ohsu.edu

Keywords

MAIT cells, MAIT cell ligands, MR1-restricted T cells, antigen presentation, cellular immune response, mucosal immunology, T-cell

Abstract

MR1-restricted T cells have been implicated in microbial infections, sterile inflammation, wound healing and cancer. Similar to other antigen presentation molecules, evidence supports multiple, complementary MR1 antigen presentation pathways. To investigate ligand exchange pathways for MR1, we used MR1 monomers and tetramers loaded with 5-(2-oxopropylideneamino)-6-d-ribitylaminouracil (5-OP-RU) to deliver the antigen. Using MR1-deficient cells reconstituted with wild-type MR1 or MR1 molecules that cannot bind 5-OP-RU, we show that presentation of monomer-delivered 5-OP-RU is dependent on cellular MR1 and requires the transfer of ligand from the soluble molecule onto MR1 expressed by the antigen presenting cell. This mode of antigen delivery strengthens the evidence for post-ER ligand exchange pathways for MR1, which could represent an important avenue by which MR1 acquires antigens derived from endocytosed pathogens.

Introduction

MR1-restricted T (MR1T) cells respond to small molecule antigens presented in the context of MHC I-related protein 1 (MR1) and include mucosal associated invariant T (MAIT) cells, which express the canonical *TRAV1-2* T cell receptor (TCR) alpha chain[1]. They are increasingly being recognized for their role in early responses to microbial infection, but also in non-infectious conditions including a variety of autoimmune disorders, wound healing and cancer (reviewed e.g. in [1,2]). Despite the heightened interest in these donor-unrestricted T cells, the mechanisms governing the presentation of MR1T cell antigens remain incompletely defined.

Successful antigen presentation requires the antigen presenting molecule to leave the endoplasmic reticulum (ER), bind an antigen, and display the bound antigen at the cell surface for TCR recognition. How these three features are achieved mechanistically, what compartments they take place in, and in what sequence they occur differs substantially between antigen

53 presentation pathways. For major histocompatibility complex (MHC) I/peptide complexes,
54 antigen binding generally precedes, and is indeed required for, ER egress and followed by
55 translocation to the cell surface (reviewed e.g. in [3]). MHC II and CD1 molecules, by contrast, exit
56 the ER bound to a surrogate ligand which is exchanged for antigenic ligand in the endosomal
57 compartment after internalization from the cell surface (reviewed e.g. in [4,5]).

58 For MR1, an MHC I-like mode of antigen acquisition has been described in which more MR1
59 associates with β_2-microglobulin and acquires endoglycosidase H resistance upon addition of
60 ligand to the culture medium[6,7]. In line with this, McWilliam, Mak, et al. have used a fluorescently
61 labelled MR1 antigen analogue to directly demonstrate loading of exogenous ligand in the ER[7].
62 Studies have linked the mechanism for MR1 ER egress to the charge neutralization of a lysine
63 residue within the MR1 ligand binding groove, which has been suggested to result in a
64 conformational change conducive to ER egress[6,7]. The most potent MR1 ligand described to date,
65 5-OP-RU, forms a Schiff base with this lysine residue, resulting in its neutralization[6,8].

66 In addition, recent findings support the hypothesis that there are complementary, non-exclusive
67 presentation pathways for MR1, allowing the molecule to survey diverse intracellular
68 compartments[9-14]. Multiple lines of evidence suggest that ligand exchange can occur on pre-
69 loaded MR1 molecules and that this may take place in an endosomal compartment. Most
70 notably, releasing MR1 from the ER prior to antigen exposure by pre-incubation with the MR1
71 ligand 6-formylpterin (6-FP) enhances presentation of exogenous antigenic ligand to MR1T
72 cells[10]. In line with this, reduced expression of proteins involved in the trafficking and recycling
73 of endosomal vesicles such as VAMP4, Rab6[9], syntaxin-4, syntaxin-16, and VAMP2[10] impairs MR1-
74 mediated antigen presentation. Based on these observations, we and others have proposed
75 ligand exchange in a post-ER compartment as a complementary mechanism for MR1 ligand
76 acquisition[6,10,11,14]. In a mechanism akin to MHC II and CD1 molecules, we hypothesize that MR1
77 molecules internalized from the cell surface can be re-loaded with microbial antigens in the
78 endosomal compartment and recycle to the cell surface to activate MR1T cells. Here we
79 investigate the mechanisms underlying MR1 ligand exchange using a novel delivery method for
80 MR1T cell antigens. We find that MR1 ligands are efficiently presented when delivered in the

81 context of soluble MR1 molecules. This presentation is dependent on host MR1 and involves the
82 transfer of antigen from the recombinant molecule onto MR1 protein expressed by the cell.
83 Building upon our previously described tetraSPOT assay[15], this method, the exSPOT, extends the
84 tool box available to investigate MR1 biology and provides important insights into the
85 mechanisms of MR1-mediated antigen presentation.

86 Results

87 *MR1 ligands delivered to antigen presenting cells on soluble MR1 molecules are efficiently*
88 *recognized by an MR1T cell clone*

89 The MR1 ligand 5-OP-RU is inherently unstable in aqueous environments[8,16], which presumably
90 includes the intracellular milieu. However, the formation of a covalent bond with the lysine
91 residue at position 43 of MR1 stabilizes the antigen[8]. We have successfully used such MR1/5-OP-
92 RU complexes in their tetramerized form in plate-bound assays to activate MR1T cells[15]. Similarly,
93 Priya and Brutkiewicz have used latex beads coated with MR1/5-OP-RU complexes to expand and
94 activate human MAIT cells[17]. While these studies used recombinant MR1 molecules immobilized
95 on a scaffold, here we sought to improve the efficiency of ligand delivery into physiologically
96 relevant antigen presenting cells (APCs) using soluble MR1.

97 To test this system, we incubated human dendritic cells (DCs) with MR1 tetramers loaded with
98 the canonical ligand 5-OP-RU (exSPOT), or applied the same concentration of tetramer directly
99 to the ELISPOT plate prior to adding an MR1T cell clone (tetraSPOT). Intriguingly, the MR1T cells
100 readily produced interferon-γ (IFN-γ) in response to the DCs incubated with soluble MR1/5-OP-
101 RU in a dose-dependent manner (Figure 1a). As expected based on previous work[15], they also
102 produced IFN-γ in the tetraSPOT. A quantitative comparison between the two assays was not
103 possible due to unknown coating efficiency in the tetraSPOT. MR1T cells did not respond to the
104 MR1/6-FP tetramer in the tetraSPOT, but we observed MR1T responses to the MR1/6-FP
105 tetramers incubated with DCs at the highest concentrations (Figure 1a). Similar to the
106 tetraSPOT[15], MR1T cell activation by DCs incubated with soluble MR1 tetramers was dependent
107 on MR1, as blocking with the anti-MR1 antibody clone 26.5 markedly reduced the response

108 (Figure 1b, EC_{50} of 0.95 pM *vs* 31.62 pM, p<0.0001). Thus, 5-OP-RU delivered in the context of
109 soluble, recombinant MR1 is efficiently presented by DCs and activates a human MR1T cell clone
110 in an MR1-dependent manner.

111 As professional APCs, DCs are particularly well equipped for phagocytosis of particulates of
112 various sizes and cross-presentation[18]. To investigate whether such specific functionality was
113 required in the exSPOT, we incubated the monocytic cell line THP-1, a B cell line (LCL), or the
114 airway epithelial cell line BEAS-2B with MR1/5-OP-RU tetramers and quantified IFN-γ responses.
115 As with DCs, the MR1T cell clone produced IFN-γ in response to all of the tetramer-incubated cell
116 types (Figure 1c). However, DCs were nearly three orders of magnitude more efficient at
117 presenting the antigen compared to the other cell types (EC_{50} of 0.55 pM *vs* 142 – 265 pM,
118 p<0.0001).

119 *Ligand delivered in the context of MR1 monomer is presented more efficiently than free ligand*

120 Next, we compared the presentation of MR1/5-OP-RU tetramers and MR1/5-OP-RU monomers
121 to reduce the variability associated with tetramerization (e.g. biotinylation efficiency,
122 streptavidin binding, and ligand saturation). Using the MR1 monomer further circumvented
123 potential variability introduced by instability of the tetramer complex over time.

124 To our surprise, presentation of ligand from monomer-incubated DCs to MR1T cells was even
125 more efficient than presentation of ligand from tetramer-incubated DCs, when accounting for
126 valency (Figure 2a). Although the EC_{50} values of the complexes were comparable (Tetramer EC_{50}:
127 0.204 pM *vs* Monomer EC_{50}: 0.22 pM, p=0.7517), there was a marked difference in the estimated
128 EC_{50} for 5-OP-RU which takes into account that each tetramer carries up to four 5-OP-RU
129 molecules whereas each monomer carries one at most (Tetramer 5-OP-RU EC_{50}: 0.816 pM *vs*
130 Monomer 5-OP-RU EC_{50}: 0.22 pM, p<0.0001). Comparing monomer-delivered 5-OP-RU to free
131 ligand further revealed improved efficiency of the monomer over the unbound antigen (Figure
132 2a; Monomer EC_{50}: 0.22 pM *vs* Free EC_{50}: 4.97 pM, p<0.0001). Of note, these calculations assume
133 full occupancy of monomers and tetramers.

134 To further investigate the relative efficiency of loading free *vs* monomer-bound 5-OP-RU, we
135 wanted to specifically detect MR1 molecules bearing 5-OP-RU at the cell surface by flow
136 cytometry. To this end, we generated a TCR tetramer based on the TCR sequence of the same
137 previously characterized MR1T cell clone that was used in the functional assays (*TRAV1-2*$^{+}$ clone
138 D426-G11 – see references[15,19]). We confirmed that this reagent specifically stained MR1
139 molecules loaded with 5-OP-RU but not 6-FP (Supplementary Figure 1). When we incubated
140 BEAS-2B cells overexpressing green fluorescent protein (GFP)-tagged MR1 (BEAS-2B.MR1-GFP)
141 with either MR1/5-OP-RU monomer or free 5-OP-RU overnight and stained with the TCR
142 tetramer to track the cell surface translocation of MR1 bound to the antigen, almost 100-fold
143 higher concentrations of free 5-OP-RU were needed to reach cell surface levels comparable to
144 monomer-delivered ligand (Figure 2b). Together, these results demonstrate that soluble,
145 recombinant MR1 is an efficient mechanism for delivery of MR1T cell antigens in a variety of cell
146 lines *in vitro.*

147 *Presentation of MR1 ligands delivered on soluble MR1 molecules requires cellular MR1*

148 In principle, the MR1/5-OP-RU complex that interacts with the TCR in our assay could be either
149 endogenously expressed MR1 bound to 5-OP-RU from the monomer or the recombinant MR1/5-
150 OP-RU monomer itself. Thus, we tested whether endogenous MR1 was required. We incubated
151 wild-type (WT) BEAS-2B cells, *MR1*$^{-/-}$ BEAS-2B cells lacking all isoforms of MR1, and *MR1*$^{-/-}$ BEAS-
152 2B cells reconstituted with tetracycline-inducible *MR1A*[20,21] with MR1/5-OP-RU monomer and
153 used them as APCs. As expected, we detected responses to WT BEAS-2B cells incubated with
154 MR1/5-OP-RU monomers (Figure 3a (i)), but when these monomers were incubated with the
155 *MR1*$^{-/-}$ BEAS-2B cell line, the response was completely abrogated (Figure 3a (ii)). Reconstitution
156 of MR1 expression in MR1-deficient cells resulted in complete recovery of MR1T cell responses
157 to the monomer-delivered ligand (Figure 3a (iii)). These observations were confirmed in THP-1
158 cells (Figure 3b).

159 *Ligands are transferred from soluble MR1 molecules onto cellular MR1*

160 Having established that MR1 expression by the APC itself was required for presentation of
161 monomer-delivered ligand, we considered two possible scenarios: (1) dimerization or indirect

162 binding of the monomer to host MR1 at the cell surface and (2) uptake of the MR1/5-OP-RU
163 complex and transfer of the antigen from the monomer onto cellular MR1.

164 Since the MR1 molecules used to generate the ligand-loaded monomers and tetramers do not
165 contain a transmembrane domain[8], their presence on the cell surface and, hence, ability to
166 activate MR1T cells, would require lateral interactions with other membrane-bound proteins. Of
167 note, Lion and colleagues have demonstrated that a GFP-tagged version of the MR1B isoform
168 weakly associated with the MR1A isoform although that observation was considered a potential
169 technical artifact[22]. To directly investigate the presence of the monomer on the cell surface, we
170 incubated BEAS-2B.MR1-GFP cells with the biotinylated MR1/5-OP-RU monomer and stained the
171 cells with fluorophore-coupled streptavidin. We did not detect any signal from the biotinylated
172 monomer although our controls confirmed that we added sufficient monomer to induce MR1
173 surface translocation and sufficient streptavidin to detect biotinylated molecules at the cell
174 surface (Figure 4a). Interestingly, we detected a small but notable shift in total MR1 surface levels
175 after incubation with the monomer (Figure 4a (iii)). This suggests that enough 5-OP-RU ligand is
176 delivered to increase not just TCR-reactive, but overall MR1 surface levels. Together, these data
177 do not support MR1 dimer formation at the cell surface.

178 Since we could not find evidence for direct presentation by the monomer, we next tested the
179 hypothesis that the 5-OP-RU is transferred from the soluble MR1/5-OP-RU complex onto the MR1
180 expressed by the APC. First, we sought to establish whether actin-dependent internalization of
181 soluble MR1 molecules was required for the presentation of monomer-delivered 5-OP-RU. Thus,
182 we treated BEAS-2B.MR1-GFP cells with latrunculin B (LatB), a well-characterized inhibitor of
183 actin polymerization. Surface levels of 5-OP-RU-loaded MR1 were reduced in cells treated with
184 LatB as compared to the dimethyl sulfoxide (DMSO) control (Figure 4b). Of note, LatB treatment
185 also reduced surface expression of TCR-reactive MR1 in response to free 5-OP-RU
186 (Supplementary Figure 2a). Total MR1 as measured by the GFP expression was not reduced by
187 LatB treatment (Supplementary Figure 2b). We concluded that an active actin cytoskeleton is
188 required for presentation of the monomer-derived ligand. This is consistent with previous results

189 demonstrating a requirement for actin for an efficient MR1 response to *Escherichia coli*
190 *(E.coli)*[13,23] and could indicate a requirement for either internalization or intracellular trafficking.

191 Additional evidence that intracellular processing is required came from the observation that the
192 kinetics of presentation differ between monomer-delivered ligand compared to free 5-OP-RU.
193 Here, we incubated BEAS-2B.MR1-GFP cells with concentrations of MR1/5-OP-RU monomer (50
194 nM) and free 5-OP-RU (6.4 µM) that resulted in intermediate surface expression (Figure 2b) and
195 followed MR1 surface translocation over time. In agreement with McWilliam et al., who detected
196 surface expression of 5-OP-RU-loaded MR1 after 2 h[6], we saw loaded MR1 as soon as 1 h after
197 addition of the free ligand (Figure 4c). By contrast, it took 6 h for the MR1 surface expression to
198 reach comparable levels after addition of the MR1/5-OP-RU monomer (Figure 4c). These kinetics
199 are consistent with a longer time needed for internalization, processing, ligand exchange, and
200 recycling of monomer-delivered ligand compared to free 5-OP-RU.

201 To directly investigate transfer onto cellular MR1, we tested whether the MR1 expressed by the
202 APC needed to be capable of presenting 5-OP-RU or whether its presence was sufficient. We
203 reconstituted the *MR1*$^{-/-}$ BEAS-2B cell line with a CRISPR-resistant version of *MR1A* that carried
204 the R9H mutation described by Howson et al.[24]. This mutation allows stable MR1 protein
205 expression and binding of 6-FP but renders the protein incapable of presenting 5-OP-RU ([24] and
206 Supplementary Figures 3 and 4). Indeed, reconstituting the MR1-deficient cells with this mutant
207 did not rescue the presentation of either monomer-delivered 5-OP-RU or *Mycobacterium*
208 *smegmatis (M. smegmatis)* supernatant (Figure 4d), further supporting the idea that it is the
209 cellular MR1 that presents the 5-OP-RU ligand.

210 *Ligand exchange occurs in post-ER compartments and does not require acidification*

211 Our data demonstrate the transfer of monomer-delivered 5-OP-RU onto MR1 expressed by the
212 APC but the mechanism of this exchange is unclear. Our lab has previously shown that pre-
213 incubation with the non-stimulatory ligand 6-FP can increase MR1-mediated antigen
214 presentation, presumably by increasing the pool of MR1 molecules available for ligand
215 exchange[10]. When we applied this concept to the monomer delivery assay, we found a similar

216 effect: releasing MR1 from the ER by pre-incubation with 6-FP decreased the EC_{50} for
217 presentation of monomer-delivered ligand from 1.027 pM to 0.1365 pM ($p<0.0001$; Figure 5a).
218 Thus, MR1 molecules pre-loaded with a non-stimulating ligand appear to contribute to the
219 activation of MR1T cells after delivery of antigenic ligand on monomers, supporting the notion of
220 ligand exchange. In this context, it is worth noting that 6-FP concentrations multiple orders of
221 magnitude higher were required to inhibit 5-OP-RU presentation in a functional assay[25], which
222 suggests stronger binding of 5-OP-RU[6] and may help push the equilibrium towards binding of the
223 activating ligand.

224 To probe to what extent the monomer delivery could be extended to other antigen presentation
225 pathways and potentially gain mechanistic insights from any parallels, we repeated the assay
226 with peptide-loaded MHC I and II tetramers. We first used a fluorophore-conjugated HLA-
227 B*08:01/CFP10$_{3-11}$ tetramer to stain a CD8$^+$ T cell clone restricted by this MHC I/peptide complex
228 (D480-F6 – see references [26] and [27]) for flow cytometry, confirming the T cell clone reacted with
229 the tetramer (Figure 5b). However, using the same tetramer to load autologous DCs in an ELISPOT
230 with the same T cell clone did not result in the production of IFN-γ in an APC-dependent manner
231 (Figure 5c). As expected, the T cells responded to DCs incubated with free peptide (Figure 5c).
232 Next, we tested an HLA-DRB1*14:03/ESAT6$_{73-78}$ tetramer in combination with a T cell clone that
233 was specific to the antigen but restricted by a different MHC II allele (D481-D1, from an HLA-
234 DRB1*14:03 negative individual). As expected, this tetramer did not stain the T cell clone by flow
235 cytometry (Figure 5d). Nevertheless, feeding the non-matched tetramer to DCs autologous to the
236 same MHC II-restricted T cell clone elicited an IFN-γ response (Figure 5e). The only source of
237 matched MHC II molecules in this case are the DCs, further supporting a requirement for transfer
238 of the antigen from the soluble protein onto antigen presenting molecules expressed by the APC
239 itself. In line with this, the T cells did not respond when using HLA-mismatched DCs or the A549
240 cell line which express MHC II alleles different from Donor 481 ([28], Cellosaurus cell line A-549
241 (CVCL_0023) (expasy.org)) (Figure 5f). Thus, like with MR1, presentation of the MHC II antigen
242 delivered in the context of recombinant antigen presenting molecules requires transfer onto
243 proteins expressed by the APC.

244 Since soluble proteins could efficiently deliver peptide for MHC II presentation, we reasoned that
245 the MR1 loading in our assay was similar to the MHC II pathway, which involves exchange of a
246 surrogate ligand in an endosomal compartment (reviewed e.g. in [4]). To test whether MR1 ligand
247 transfer from the monomer could be mediated in an analogous fashion, we investigated the
248 effect of brefeldin A (BFA) on the presentation of monomer-delivered 5-OP-RU. BFA disrupts the
249 Golgi apparatus and effectively traps secretory proteins in the ER. Indeed, incubation with BFA
250 diminished surface translocation of 5-OP-RU-loaded MR1 in response to the MR1/5-OP-RU
251 monomer (Figure 5g). However, this experiment is unable to distinguish between two different
252 scenarios: 1) ligand exchange occurs in the ER and MR1 needs to subsequently traverse the Golgi
253 for surface presentation, or 2) MR1 needs to leave the ER to be available for exchange in a post-
254 ER compartment. To distinguish between these two hypotheses, we pre-incubated the cells with
255 6-FP to induce ER egress of a pool of MR1 molecules before adding the BFA. Under these
256 conditions, BFA had a minimal effect on presentation of monomer-delivered ligand (Figure 5g).
257 As expected, presentation of free 5-OP-RU was similarly impaired in the presence of BFA and
258 improved after pre-incubation with 6-FP (Supplementary Figure 5). It is important to note that
259 BFA treatment also reduced total MR1 levels as measured by GFP expression (Figure 5g). These
260 data clearly show that 5-OP-RU delivered on soluble, recombinant MR1 molecules can be
261 transferred to cellular MR1 in a post-ER compartment.

262 To further characterize the compartment where ligand exchange in the exSPOT occurs, we
263 performed immunofluorescence microscopy. We observed AF647-labeled MR1/5-OP-RU
264 tetramer in compartments labeled with Rab5 (23.51%, standard deviation (SD) = 11.93), an early
265 endosome marker, or LAMP1 (33.1%, SD=12.3), which localizes to late endosomes and lysosomes
266 in these cells (Figure 6a). These observations support the hypothesis that ligand transfer occurs
267 in post-ER compartments, including the early and late endosome.

268 Exchange of exogenous ligand onto MHC II[4] and CD1[5] molecules is potentiated by the low pH in
269 the endolysosomal compartment. Pertinently, endosomal acidification is required for efficient
270 presentation of *E. coli* by MR1 [13,29] and McWilliam et al. have proposed that the Schiff base that
271 links 5-OP-RU to the MR1 ligand binding groove is labile under acidic conditions[6,14]. Therefore,

272 we investigated whether presentation of monomer-delivered ligand was dependent on
273 endosomal acidification. We pre-incubated BEAS-2B WT cells with bafilomycin before performing
274 the exSPOT. Bafilomycin inhibits vacuolar ATPases[30] and diminishes the presentation of an
275 endosomal processing-dependent 5-A-RU pro-drug to MR1T cells[12]. Whereas the bafilomycin
276 concentrations we used here reduced the MR1T cell response to this pro-drug in a dose-
277 dependent manner, presentation of the monomer-delivered 5-OP-RU was not affected by the
278 inhibitor (Figure 6b). Together, these data support a model in which the transfer of 5-OP-RU
279 delivered in the context of a soluble MR1 monomer onto the MR1 expressed by the APC can
280 displace pre-bound 6-FP and is independent of endosomal acidification.

281 Transfer of monomer-bound 5-OP-RU requires breaking a covalent bond. Since acidification was
282 not needed for ligand transfer (Figure 6b), we hypothesized that this process is catalyzed by an
283 exchange chaperone akin to HLA-DM for MHC II[4,31]. TAPBPR, tapasin, and the adapter protein
284 AP2A1 have been shown to bind MR1 and modulate its antigen presentation[7,32,33]. However,
285 knock down (KD) of these candidate chaperones alone or together did not affect how efficiently
286 monomer-delivered 5-OP-RU was presented to our MR1T cell clone (Supplementary Figure 6).

287 Vesicular trafficking between the cell surface and the endosomal compartments is mediated by
288 soluble N-ethylmaleimide-sensitive factor attachment protein receptors (SNAREs)[34]. The SNARE
289 syntaxin-4 (encoded by *STX4*) is required for exocytosis in various cellular contexts[35-38] including
290 the fusion of recycling endosomes to the plasma membrane in cytotoxic T cells[35] and post-
291 synaptic membranes on dendritic spines[36]. Our lab has previously shown that small interfering
292 RNA-mediated knock down of *STX4* reduces MR1-mediated antigen presentation of *M.*
293 *smegmatis* supernatant but not live *Mycobacterium tuberculosis*[10]. To investigate the
294 involvement of this mediator of vesicular trafficking in the exSPOT, we generated BEAS-2B cells
295 deficient for *STX4* using CRISPR/Cas9 technology. Consistent with previous results in the knock
296 down system[10], *STX4* KO cells presented *M. smegmatis* supernatant less efficiently than their
297 Cas9-expressing parent cell line (Figure 6c, $p<0.0001$). Similarly, presentation of monomer-
298 delivered antigen was reduced in the absence of the SNARE (Figure 6c, $p=0.0032$). These results

299 implicate syntaxin-4 in the mechanism underlying the exSPOT and suggest that it may share
300 mechanistic parallels with presentation of microbial ligand.

301 Discussion

302 Distinct and complementary cellular pathways have been proposed for MR1 loading and
303 trafficking[11,14,39,40]. While most research efforts have been focused on the ER pathway, increasing
304 evidence supports exchange in a post-ER compartment as a mechanism by which MR1 acquires
305 antigenic ligand(s). For example, both Karamooz et al. and McWilliam et al. have shown that MR1
306 molecules in cells pre-incubated with the MAIT cell antagonist 6-FP can present activating MR1
307 ligands upon subsequent incubation with agonistic antigen[6,10]. Pre-treatment with 6-FP counters
308 the ability of BFA to block surface expression of MR1/5-OP-RU complexes, indicating re-loading
309 in a post-ER compartment[6]. Indeed, pre-incubation with 6-FP enhances MR1-mediated
310 presentation of bacterial supernatant, presumably by increasing the pool of MR1 molecules
311 available for re-loading[10]. Using a fluorescence internalization probe, McWilliam et al. also
312 directly demonstrated recycling of a small proportion of MR1 molecules[6]. Furthermore, a
313 recently developed pro-drug requires endosomal processing to release the 5-OP-RU precursor 5-
314 A-RU[12]. Since the antigen is generated in endosomes in this scenario, it appears likely that the
315 ligand is loaded onto MR1 in this compartment as opposed to trafficking to another intracellular
316 organelle, which would require it to cross multiple membranes. Interestingly, while Ac-6-FP
317 inhibits T cell activation after delivery of free 5-A-RU, it does not interfere with the presentation
318 of this pro-drug[12]. This is consistent with the earlier observation that 6-FP blocks presentation of
319 bacterial supernatant but not of intracellular infection[9]. The same study demonstrated that MR1-
320 mediated antigen presentation of *M. smegmatis* supernatant is reduced upon knock-down of
321 endosomal trafficking molecules[9,10], further supporting involvement of this pathway in efficient
322 loading of some antigens. In addition, a synthetic MR1 ligand modified to be able to track its
323 location by microscopy resides in small vesicles also occupied by the micropinocytosis marker
324 dextran[7]. This supports the idea that both membrane-bound internalized MR1 and soluble MR1
325 ligands could occupy this compartment at the same time, facilitating loading[14]. Together, these
326 data lead us to hypothesize that there are distinct pools of MR1 in the ER and in a post-ER

327 compartment[11,12,14,40], that these compartments are differentially accessed by exogenous
328 ligands, and/or that conditions are more favorable for ligand exchange in the endosomal
329 compartment than in the ER. This notion is not without precedent as multiple, complementary
330 pathways including both direct loading in the ER and ligand exchange in the endosomal
331 compartment have been shown for MHC I (reviewed e.g. in [41]).

332 In this study, we report a delivery method for MR1 ligands which allowed us to directly
333 demonstrate transfer of the MR1T cell-activating ligand 5-OP-RU from recombinant, soluble MR1
334 onto cellular MR1. Intriguingly, monomer-delivered antigen was presented more efficiently than
335 tetramer-delivered ligand. We speculate that the bulky structure of the tetramer may result in
336 steric hindrance of interactions with chaperones required for ligand transfer. The smaller, more
337 compact monomer, on the other hand, may be better suited to adopt the correct orientation.
338 Moreover, DCs were much more efficient at presenting the tetramer-derived ligand than other
339 cell lines tested. This could be due to their ability to cross-present internalized antigen, which
340 allows their MHC I molecules to sample diverse sources of antigen and may enable MR1 to do
341 likewise[18].

342 Monomer-delivered 5-OP-RU was also presented to MR1T cells more efficiently than free 5-OP-
343 RU. One explanation for this observation is that binding to the monomer protects the inherently
344 unstable antigenic molecule from dehydrative cyclization[8]. However, the analogous results with
345 MHC II tetramers argue that the enhanced antigen presentation associated with monomer
346 delivery is not simply attributable to increased stability as peptide antigens are more stable.
347 Therefore, we think it more likely that the monomer delivery enhances the efficiency of
348 presentation by improving another aspect of antigen processing or presentation.

349 Previous 6-FP pre-loading experiments suggested that MR1 ligand exchange requires
350 internalization of the antigen presentation molecules as it did not occur if cells were incubated
351 at 4°C[6]. Interestingly, recent data from a similar model indicated that internalization mediated
352 by the adapter protein AP2A1 is not required for the exchange of 6-FP for an MR1 ligand linked
353 to a fluorophore[33]. While ligand exchange may occur on the cell surface in this model, the data
354 presented in this manuscript support the conclusion that internalization of the ligand-loaded

355 monomer is required for the exSPOT (Figure 4a-c; Figure 6a). Thus, it appears unlikely that the
356 ligand exchange in this delivery method could occur at the plasma membrane.

357 Our efforts to identify the molecular mechanism that enables transfer of the antigenic ligand
358 from the soluble MR1 to the cellular MR1 show that this process is dependent on actin dynamics
359 and enhanced if cellular MR1 is pre-loaded with 6-FP. Peptide editing on MHC I and MHC II
360 depends on the relative affinities of the available ligands and their competition for transiently
361 ligand-receptive antigen presenting molecules[3,4,31]. In line with this concept, we propose that the
362 endosomal compartment is a uniquely suited place for MR1 ligand exchange by virtue of its high
363 local concentration of antigens derived from internalized pathogens relative to the cell as a
364 whole. This enrichment of otherwise low abundance ligands may drive the equilibrium from pre-
365 bound ligands to internalized antigens specifically in endosomal compartments.

366 This analogy breaks down, however, in that peptides are not covalently bound to their antigen
367 presenting molecules. By contrast, a covalent bond needs to be broken in our exchange assay to
368 release the antigenic ligand from the soluble MR1. The Schiff base that anchors both 6-FP and 5-
369 OP-RU to the MR1 binding groove is considered labile under acidic conditions[6,14]. Nevertheless,
370 our results suggest that ligand exchange on MR1 does not require endosomal acidification. This
371 is in striking contrast to MR1-mediated presentation of fixed whole *E. coli*[13] and the 5-A-RU pro-
372 drug[12]. While the latter was designed to require acidic conditions for release, the first suggests
373 that the molecular mechanisms for MR1 loading differ between *E.coli* and 5-OP-RU-loaded
374 monomer. Importantly, *Mycobacterium tuberculosis* is known to prevent endosomal acidification
375 to evade immune recognition[42], making antigen loading mechanisms that function at higher pH
376 desirable. Alternatively, ligand transfer after monomer delivery may be insensitive to bafilomycin
377 because it occurs in the ER. Previous studies have demonstrated that whole proteins from the
378 extracellular environment can be imported into this compartment[43-45], so this may be true for
379 the MR1 monomer, too. In that case, we would, however, expect monomer delivery to efficiently
380 supply ligand to MHC I molecules as well, which is not the case (Figure 5c). Our BFA experiments
381 also show that MR1 ligand exchange can take place after MR1 is released from the ER bound to
382 6-FP (Figure 5g).

383 While the molecular mechanism and the subcellular location of ligand exchange remain to be
384 determined, our data lead us to propose that it is a facilitated process catalyzed by a yet
385 unidentified exchange chaperone (Supplementary Figure 7). Monomer delivery may increase the
386 efficiency of exchange by enhancing the interaction between pre-loaded MR1 and this
387 chaperone. Indeed, specific chaperones facilitate the release of pre-loaded ligands, stabilize the
388 transiently unoccupied antigen presenting molecule, and mediate the re-loading with antigenic
389 cargo in other examples of ligand exchange. For MHC I, for instance, this function can be fulfilled
390 by TAPBPR in the Golgi (reviewed e.g. in [46] and [47]). For MHC II, HLA-DM chaperones endosomal
391 ligand exchange and exchange kinetics are further modulated by its regulator HLA-DO (recently
392 reviewed in [31] and [4]). Recent screens for modulators of MR1 loading and trafficking have
393 identified numerous interaction partners through both genetic techniques and protein co-
394 immunoprecipitation[7,48]. These studies found MR1-mediated antigen presentation to be
395 regulated by tapasin and TAPBPR[7,32] and the P5-type ATPase ATP13A1[48], but have largely focused
396 on ER and Golgi-resident proteins. Discovery approaches more specifically targeted at interaction
397 partners during ligand exchange in endosomal compartments may be needed to identify the
398 chaperone(s) involved in this process.

399 In this manuscript, we explored the mechanisms by which MR1 ligands can be delivered
400 exogenously using MR1 itself to stabilize an inherently unstable ligand. This mode of ligand
401 delivery is a powerful tool to identify chaperones involved in the re-loading of pre-loaded MR1
402 molecules which can then be tested for their involvement in physiological settings such as
403 mycobacterial infection. 5-OP-RU was also recently successfully used to boost mucosal immunity
404 in the context of vaccinations against respiratory pathogens[49]. Thus, in addition to its use in
405 exploring the molecular underpinnings of ligand exchange, we also postulate MR1/ligand
406 complexes could be used as an adjuvant or antigen delivery strategy in vaccination approaches.

407 Methods

408 *Human subjects*

409 This study was conducted according to the principles expressed in the Declaration of Helsinki.
410 Study participants, protocols, and consent forms were approved by the Institutional Review

411 Board at Oregon Health & Science University (OHSU) (IRB00000186). All ethical regulations
412 relevant to human research participants were followed. Peripheral blood mononuclear cells
413 (PBMC) from human subjects were only used to make dendritic cells to be used as antigen
414 presenting cells or used to expand T cell clones as described in the methods section. All findings
415 in this manuscript are based on the T cell clone function or on other cell line function, e.g. BEAS-
416 2B cell line. No data is presented on the PBMC from human subject participants and sex and
417 gender were not taken into consideration.

418 *Cells and bacteria*

419 *M. smegmatis* (strain mc^{2}155) supernatant was obtained by growing *M. smegmatis*, centrifuging
420 the cultures and filtering the supernatant through a syringe-driven 0.22 µm filter[10]. PBMCs were
421 isolated from whole blood obtained by leukapheresis with informed consent. Human monocyte-
422 derived dendritic cells (DCs) were isolated from PBMCs by plate adherence. For this, PBMCs were
423 incubated in RPMI supplemented with 2% heat-inactivated human serum, 3.5 mM L-Glutamine
424 (gibco), and 44 µg/ml gentamycin (gibco) at 37°C for 1h, before gentle tapping and removal of
425 non-adherent cells. Adherent cell were then cultured in RPMI supplemented with 10% heat-
426 inactivated human serum and L-Glutamine and gentamycin as above (RPMI10%HuS) and 30
427 ng/ml GM-CSF (Immunex) and 10 ng/ml IL-4 (R&D Systems) for 5 days[50]. BEAS-2B cells were
428 obtained from the American Type Culture Collection (ATCC) and cultured as recommended.
429 These cell lines are passaged up to 15 times before being discarded. Freezebacks are frozen down
430 during the first 2-3 passages and are routinely tested for mycoplasma. BEAS-2B *MR1*$^{-/-}$, BEAS-2B
431 *MR1*$^{-/-}$: *MR1A*[20,21] and the BEAS-2B cell lines overexpressing GFP-tagged MR1A constitutively
432 (BEAS-2B.MR1-GFP)[51] or under the tetracycline-inducible promoter[52] were described previously.
433 THP-1 cells were obtained from ATCC. THP-1 *MR1*$^{-/-}$ and THP-1 *MR1*$^{-/-}$: *MR1* cell lines were
434 described previously[21,53]. The THP-1 *MR1*$^{-/-}$ from the Sewell lab constitutively express Cas9
435 protein whereas the THP-1 *MR1*$^{-/-}$: *MR1* cells from the Cerundolo lab do not. EBV-transformed B
436 cell lines (LCL) were generated in our laboratory using supernatants from the cell line 9B5–8
437 (ATCC). A549 cells were obtained from ATCC. The pCI AscI MR1 R9H res construct (Addgene ID
438 214753) was based on work by Howson et al.[24]. pCI AscI MR1 res (Addgene ID 214752) and pCI
439 AscI MR1 R9H res (Addgene ID 214753) contain silent mutations to make the sequence resistant

440 to CRISPR/Cas9 editing in the *MR1*$^{-/-}$ background. For both plasmids, the coding sequence with a
441 downstream internal ribosomal entry site (IRES) GFP[54] was ordered from GeneArt (ThermoFisher)
442 and cloned into our previously described pCI AscI vector[10]. Plasmids were sequenced at the OHSU
443 sequencing core and transfected into BEAS-2B *MR1*$^{-/-}$ cells using the Amaxa nucleofection system
444 with Kit T solution (Lonza). The transfection efficiency was evaluated via GFP expression by flow
445 cytometry (Supplementary Figure 4). *Trichoplusia ni* (Hi-5, Thermo Fisher Scientific) and
446 *Spodoptera fugiperda* (Sf9, Thermo Fisher Scientific) cells for baculovirus production and
447 recombinant protein expression were maintained as described previously[55].

448 *CRISPR/Cas9-mediated knock out of STX4*

449 To generate knockout cells, we used a two-plasmid system in which both the Cas9 gene and the
450 sgRNA were cloned into different lentiviral vectors with independent selection markers similar
451 to the method used by Niekamp et al. [56]. The plasmids used for the generation of lentivirus
452 comprise the lentiviral vector (pCDH-sgRNA or pCW-Cas9), the psPAX2 (packaging), and the
453 pMD2.G (envelope) plasmids. The pCW-Cas9 plasmid was obtained from Addgene (#50661), as
454 were psPAX2 (Addgene #12260) and pMD2.G (Addgene #12259). Lentiviruses were generated by
455 transfecting low-passage HEK293T cells with these plasmids. Early passage BEAS-2B WT cells
456 were stably transduced with these lentiviral particles encoding Cas9 by spinoculation[57].
457 Transduced cells were selected by culturing with 5 µg/ml Blasticidin (Life Tech) for 12 days. Three
458 sgRNA constructs targeting *STX4* were generated using the sgOpti plasmid (Addgene ID 85681)
459 as a backbone and packaged into lentiviral particles[58]. Early passage BEAS-2B.Cas9 cells were then
460 transduced with supernatant containing these lentiviral particles in the presence of 200 µg
461 Polybrene (Sigma). Transduced cells were selected by culturing with 8 µg/ml Puromycin (Sigma)
462 for 6 days. Monoclonal populations were created by limiting dilution and a functional screen was
463 performed by ELISPOT. Genomic editing efficiency and clonality were verified by Sanger
464 sequencing. Briefly, DNA was isolated from *STX4* KO clones and BEAS-2B.Cas9 control cells using
465 the QIAamp DNA Micro Kit (Qiagen) per manufacturer's protocols. DNA surrounding the sgRNA
466 target site was amplified by PCR (STX4-1F: ACAAGGTGGTTAAGGTGGCA; STX4-1R:
467 CTGTTCACAGGGAGACCGAC) and purified using the QIAquick PCR Purification Kit (Qiagen) per
468 manufacturer's protocols. Sanger sequencing was performed by capillary electrophoresis at the

469 OHSU Vollum Institute DNA Sequencing Core and sequences were analyzed by Tracking of Indels
470 by DEcomposition (TIDE)[59] and Inference of CRISPR Edits (ICE)[60]. Sequence of the sgRNA used to
471 generate the *STX4* KO clonal cell line used in this manuscript: AGAACGTGGAGCGGATTCGG.

472 *T cell clones*

473 T cell clones were expanded by co-culture with irradiated allogeneic PBMC and irradiated LCL in
474 RPMI10%HuS in the presence of anti-CD3 antibody (Thermo Fisher Scientific, clone OKT3, Cat No.
475 16-0037-81, used at 30 ng/ml)[19,26]. Recombinant interleukin-2 (Proleukin, OHSU Inpatient
476 Pharmacy) was added to the cultures every 2-3 days to a final concentration of 2 ng/ml and anti-
477 CD3 antibody was washed off on Day 5. T cells were frozen down at -80°C at 1e6/ml after at least
478 11 days and used from frozen. T cell clones are expanded from frozen stocks using published
479 protocols and are used for 2 weeks and then discarded. They are also tested to confirm their
480 phenotype using either ELISPOT or flow cytometry and routinely tested for mycoplasma. Three T
481 cell clones were used in this work. Two clones have been published previously (D426-G11[15,19] and
482 D480-F6[26,27]). D481-D1 is a $CD4^+$ T cell clone that recognizes $Esat6_{73-87}$. This clone was generated
483 in a limiting dilution assay by adding either 100, 200 or 600 $CD4^+$ T cells (CD4 microbeads,
484 Miltenyi) isolated from PBMC from D481, a participant who had active tuberculosis, to wells of a
485 96 well plate containing 1e5 irradiated (3,500 rad using a Cs source) allogeneic PBMCs, 1e4
486 irradiated (3,500 rad using a Cs source) autologous dendritic cells (prepared as described above),
487 2 µg/ml Esat6 protein (BEI Resources), 5 ng/ml interleukin-2 and incubated at 37°C for two weeks.
488 Wells with growth were assessed for response to an Esat6 peptide pool consisting of 15mers
489 overlapping by 11 amino acids in an IFN-γ ELISPOT. T cell clones that responded to the Esat6
490 peptide pool were expanded as described above[19,26] and further screened against the individual
491 15mers. The restricting allele is not known for this clone, but D481 expresses these class II alleles:
492 DRB1*08:01, DRB1*13:01, DPB1*01:01, DPB1*04:01, DQB1*04:02 and DQB1*06:03 (HLA typing
493 by Kashi Clinical Laboratories, Portland, OR).

494 *ELISPOT assays*

495 For the plate-bound tetramer ELISPOT (tetraSPOT) assay, ELISPOT plates were coated with 50 µl
496 of anti–IFN-γ antibody (Mabtech, clone 1-D1K, Cat No. 3420-3-1000, used at 10 µg/ml) per well.

497 At the time of coating, MR1/5-OP-RU and MR1/6-FP tetramers conjugated to PE obtained from
498 the NIH tetramer core[8] were added at a range of concentrations. After overnight incubation at
499 4°C, ELISPOT plates were washed three times with phosphate-buffered saline (PBS) and then
500 blocked with RPMI10%HuS for at least 1 h. T cell clones (1e3-2e4) were added to wells overnight.
501 IFN-γ ELISPOTs were enumerated following development with an alkaline phosphatase-
502 conjugated secondary antibody (Mabtech, clone 7-B6-1-ALP, Cat No. 3420-9A-1000, used
503 1:1000). Briefly, ELISPOT plates were washed extensively in PBS+0.05% Tween-20 (Thermo
504 Scientific), incubated with secondary antibody for at least 2h at room temperature, washed in
505 PBS+0.05% Tween-20 again and then PBS before incubation with BCIP/NBT-plus developer
506 (Mabtech). Dried plates were imaged with an AID ELISPOT reader and spots were counted using
507 the AID ELISPOT software Version 7.0. For all other ELISPOT assays, ELISPOT plates were coated
508 with anti-IFN-γ antibody and blocked as described above. 1e4 DC, LCL, THP-1 or BEAS-2B cells
509 were plated in the ELISPOT wells in RPMI10%HuS human serum. Tetramer, monomer, ligand or
510 peptide were added to the wells at concentrations indicated for each experiment. PHA was used
511 as positive control. After at least 1 h, 1e3-2e4 T cell clones were added and the plate was
512 incubated overnight at 37°C. Antibody blocking was performed using the anti-MR1 26.5 clone
513 (OHSU antibody core) and an IgG2a isotype control (Biolegend, clone MOPC-173, Cat No. 400224)
514 added at 5 µg/ml for 1 h prior to the addition of ligand. 6-FP pre-treatment assays were
515 performed as follows[10]. BEAS-2B.MR1-GFP cells were plated in 6-well tissue culture plates and
516 treated with 6-FP *vs* NaOH control over night. On the next day, the cells were harvested and used
517 as APCs in an IFN-γ ELISPOT assay as described above. For experiments with Bafilomycin A1
518 (MedChemExpress), BEAS-2B cells were incubated with Bafilomycin A1 for 2 h at indicated
519 concentrations prior to the addition of 100 pM MR1/5-OP-RU monomer or 50 nM 5-OP-RU
520 prodrug (MedChemExpress) in an IFN-γ ELISPOT assay as described above.

521 *5-OP-RU Ligand*

522 5-(2-oxopropylideneamino)-6-d-ribitylaminouracil (5-OP-RU) was made from two sources of 5-
523 amino-6-D-ribitylaminouracil (5-A-RU). For the first method, 5-nitro-6-d-ribitylaminouracil (5-N-
524 RU) was prepared by the OHSU Medicinal Chemistry Core. 5-A-RU was freshly prepared from 5-

525 N-RU following a previously described procedure[8]. In brief, 4.8 mg of 5-N-RU was dissolved in 400
526 µl of 50 mM MES, pH 5.8. 8-fold molar excess of sodium dithionite powder was added and
527 incubated in the dark at 90°C for five minutes under argon. The solution was chilled in an ice
528 water bath. To prepare 5-OP-RU, at least 15 molar equivalents of methylglyoxal was added to 5-
529 A-RU in 100 mM HEPES, pH 7.2, 150 mM NaCl to give a stock solution at 20 mM. For the second
530 method, 5-A-RU*HCl was prepared by the OHSU Medicinal Chemistry Core following a previously
531 described procedure[61]. To prepare 5-OP-RU, equal volumes of circa 650 mM methylglyoxal
532 (Sigma) and 32 mM 5-A-RU*HCl dissolved in water were combined immediately before addition
533 to the assay to give a stock solution of 16 mM of 5-OP-RU. Mass spectrometry analysis confirmed
534 near-complete conversion of 5-A-RU into 5-OP-RU under similar conditions (Supplementary
535 Figure 8). For this, samples were directly injected into an AB Sciex TripleTOF 5600 quadrupole
536 time of flight mass spectrometer using the built-in syringe pump through a Hamilton Model 1710
537 N 100 µl syringe. Samples passing through the syringe were ionized by a PicoView ion source by
538 New Objective before passing through a Co-Ann technologies 11cm 20 µm inner diameter pulled
539 glass emitter which tapered to a 10 µm inner diameter at the tip. A stock solution of 32 mM 5-A-
540 RU was diluted 1:10 before injection into the mass spectrometer. 5-OP-RU was produced by
541 combining a 5 µl stock solution of 32 mM of 5-A-RU with a 5 µl 1:10 dilution from a 6.5 M stock
542 solution of methylglyoxal (Sigma). This 5-OP-RU was then diluted 1:10 for injection into the mass
543 spectrometer. Samples were examined in negative ion mode with the source voltage set at -2600
544 V. MS1 and MS2 data was acquired using Analyst 1.8 in manual tuning mode, with a TOF mass
545 range of 30 to 500 Da after 1 minute. MS2 data was collected in high sensitivity mode with a
546 declustering potential of -40 and a collision energy of -30 for 5-A-RU and -38 for 5-OP-RU. Data
547 was analyzed using PeakView 1.2.

548 *Flow Cytometry assays*

549 The following reagents were obtained through the NIH Tetramer Core Facility: MR1/5-OP-RU
550 tetramer and monomer and MR1/6-FP tetramer and monomer, HLA*B08:01/CFP10$_{3-11}$ tetramer,
551 HLA-DRB1*14:03/Esat6$_{73-87}$ tetramer, HLA-DRB1*14:03/control tetramer. Identification of MAIT
552 cells with MR1 tetramers was described in [8]. The D426-G11 TCR tetramer was made as specified
553 below. To confirm the specificity of the TCR tetramer as a staining reagent, BEAS-2B.MR1-GFP

554 cells were incubated with the indicated concentrations of 5-OP-RU or 6-FP, or the equivalent
555 volume of 0.01 M NaOH overnight. Cells were harvested with Trypsin and split into three wells
556 of a U-bottom 96-well plate each for staining with TCR tetramer, anti-MR1 antibody 26.5
557 (BioLegend, Cat No. 361108, used at 0.4 µg/ml), or isotype control antibody (BioLegend, Cat No.
558 400222, used at 0.4 µg/ml) for at least 30 min on ice. BEAS-2B *MR1*$^{-/-}$ cells transfected with the
559 pCI AscI MR1 res or pCI AscI MR1 R9H res plasmids were analyzed similarly. For ligand titration
560 experiments, 5e4 BEAS-2B.MR1-GFP cells per well were incubated with the indicated
561 concentrations of free 5-OP-RU or MR1/5-OP-RU monomer in a 24-well plate overnight. Cells
562 were harvested with Trypsin, transferred to a 96-well U-bottom plate, washed, and stained with
563 TCR tetramer for at least 30 min at 4° C. For time course experiments, 5e4 BEAS-2B.MR1-GFP
564 cells per well were plated in 24-well plates. Free 5-OP-RU or MR1/5-OP-RU were added to the
565 indicated final concentrations for the indicated amounts of time. Samples from all time points
566 were harvested and stained at the same time as above. Free ligand and monomer titrations were
567 performed in parallel in both sets of experiments. For the actin blockade, 5e4 BEAS-2B.MR1-GFP
568 cells were plated in 24-well plates and left to adhere overnight. Cells were then treated with 10
569 µM Latrunculin B (Sigma) or the equivalent volume of DMSO (Sigma). After 1 h, MR1/5-OP-RU or
570 MR1/6-FP monomer was added to a final concentration of 100 nM and the cells were incubated
571 for another 4 h before staining as above. For Brefeldin A blocking experiments, BEAS-2B.MR1-
572 GFP cells were incubated with 94 µM 6-formylpterin (6-FP, Schircks) or the equivalent volume of
573 0.01 M NaOH (Sigma) overnight at 37°C at 5e4/well in a 24-well plate. 6-FP was washed off and
574 the cells treated with 50 µg/ml Brefeldin A (BFA, Sigma) or the equivalent volume of DMSO
575 (Sigma) for 1 h, followed by the addition of MR1/6-FP or MR1/5-OP-RU monomer (100 nM) or
576 free 5-OPRU (5 µM) or 6-FP (100 µM) and incubation at 37°C for 4 h. Cells were then stained with
577 TCR tetramer as above. The gating strategy is shown in Supplementary Figure 9. TCR tetramer
578 was used at 150 or 300 nM. BEAS-2B WT cells were used for unstained and single color controls.
579 Anti-MHC I antibody W6/32 (BioLegend, Cat No. 311410, used at 0.64 or 2.56 µg/ml) was used
580 for the APC single color control due to low MR1 expression on BEAS-2B WT cells. For surface
581 staining of BEAS-2B.MR1-GFP cells with streptavidin, 3e5 cells were incubated with 50 nM of
582 MR1/5-OP-RU monomer or medium overnight. These cells were split into multiple wells and

583 either stained with the TCR tetramer as described above or blocked with PBS + goat, human, and
584 bovine serum for at least 30 min on ice and then stained with Streptavidin-APC (Agilent) for 40
585 min on ice or with biotinylated anti-MR1 antibody 26.5 (BioLegend, custom conjugation, used at
586 5 µg/ml) for 40 minutes on ice, followed by Steptavidin-APC for 40 minutes on ice. For tetramer
587 staining of the CD8 T cell clone D480-F6, 1e5 T cell clones were incubated with the
588 HLA*B08:01/CFP10$_{3-11}$ tetramer at 1:500 (0.127 µg/well) for 45 minutes at 37°C. For tetramer
589 staining of the CD4 T cell clone D481-D1, 1e5 T cell clones were incubated with the HLA-
590 DRB1*14:03/Esat6$_{73-87}$ or HLA-DRB1*14:03/control at 6 µg/ml for 1 h at 37°C. Cells were
591 subsequently stained with an antibody cocktail containing LIVE/DEAD Fixable Dead Cell Stain Kit
592 (Thermo Fisher), and surface stained with the antibodies to CD4 (BD Biosciences, clone SK3, Cat
593 No. 348789 or 612748, used at 2.5 or 1 µl/test, respectively), CD8 (Biolegend, clone SK1, Cat No.
594 344714, used at 0.01 µl/test), and CD3 (BD Biosciences, clone SK7, Cat No. 340663, used at 3
595 µl/test or BioLegend, clone OKT3, Cat No. 317324, used at 1 µl/test), for 30 minutes at 4°C.
596 Samples were washed and fixed with 1% PFA. Acquisition was performed using a BD
597 FACSymphony, LSRII, or Canto cytometer. The gating strategy is shown in Supplementary Figure
598 10. Flow cytometric analysis was performed using FlowJo version 10.6.1 or 10.7.1 (Treestar,
599 Ashland, OR, USA). Plots show GFP+ gates to ensure only cells over-expressing MR1 are included
600 in the analysis.

601 *Knock down of candidate chaperones*

602 For small interfering RNA-mediated knock down of candidate chaperones, small interfering
603 RNAs targeting TAPBPR (Assay ID s229969), tapasin (Assay ID 41850), or AP2A1 (Assay ID s183)
604 or a missense control (4390844) (all Thermo Fisher Scientific) were nucleofected into 1e6 BEAS-
605 2B WT cells at 300 nM according to the manufacturer's instructions (Lonza, Nucleofector Kit T).
606 Cells were allowed to rest overnight (TAPBPR and tapasin) or two days (AP2A1) before use in an
607 ELISPOT assay as described above. RNA levels of targeted transcripts were measured by qRT
608 PCR at the time of ELISPOT using Taqman probes Hs00794155_m1, Hs00917451_g1, and
609 Hs00900330_m1 with GAPDH (Hs02758991_g1) as the housekeeping gene (all Thermo Fisher
610 Scientific). For AP2A1, equal cell numbers were also lysed in Lysis Buffer (Chromotek) with

611 Protease Inhibitor cocktail (Roche) at the time of ELISPOT and lysates of all three experiments
612 were analyzed together by Western blot. Briefly, lysates were combined with Loading Buffer
613 and Reducing Agent (both Invitrogen), separated on 4-20% polyacrylamide gels (Bio-Rad), and
614 transferred onto PVDF membrane (Millipore). The membrane was blocked with Blocking Buffer
615 (Odyssey) for 1 h at room temperature before incubation with mouse anti-AP2A1 (BD, clone 8,
616 Cat No. 610501, used at 250 ng/ml) and rabbit anti-ACTB (Abcam, Cat No. ab8227, , used at 200
617 ng/ml) primary antibodies overnight at 4° C. The blot was developed with LI-COR IRDye
618 secondary antibodies (goat anti-mouse 800CW and goat anti-rabbit 680RD, Cat No. 926-32210
619 and 926-68071, both used at 100 ng/ml) and imaged simultaneously on an Odyssey imager.
620
621 *Recombinant protein expression and purification*

622 All experiments using MR1 monomer and tetramer were performed with the reagent(s)
623 provided by the NIH Tetramer Core Facility. The D426-G11 TCR was produced as previously
624 described for other MAIT TCRs[62]. Briefly, the D426-G11 TCR V(D)J region of each TCR chain was
625 cloned separately into the pAcGP67a vector after the GP67 signal sequence and before either a
626 "cysteine-optimized" TRAC or TRBC sequence[63]. To ensure heterodimer formation, the chains
627 were tagged with cleavable C-terminal acidic and basic zippers[64] each followed with a 6xHis tag.
628 The alpha chain construct contained a C-terminal AviTag before the zipper cleavage site. The P1
629 and P2 baculoviruses were produced in Sf9 cells[55], then the baculoviruses were added in
630 tandem to Hi-5 cells and the cells were allowed to express the recombinant protein for 72 h.
631 The supernatant was harvested and the protein purified by Ni-NTA chromatography.
632 Recombinant TCR was then treated with recombinant HRV 3C protease overnight and the
633 cleaved zippers were removed with Ni-NTA. The protein was biotinylated *in vitro* using
634 recombinant BirA ligase and the biotinylation efficiency checked by a streptavidin gel-shift
635 assay. Finally, it was purified by size exclusion chromatography and tetramerized with
636 streptavidin-APC (Agilent). This reagent is available upon request after the completion of an
637 MTA that includes a clear description of how the material would be used.

638 *Microscopy*

639 BEAS-2B cells (1e5) were seeded on a chamber slide and incubated for 18 h at 37C. MR1/5-OP-
640 RU tetramer conjugated to AF647 (200 nM) was added to the experimental wells for 2 h at RT.
641 Control wells received no tetramer. To determine whether the tetramer was observed in the
642 cells, CellMask Orange Plasma (1:5000 dilution, Invitrogen) was added for 10 min (Supplementary
643 Figure 11). To examine whether the tetramer localized to endosomal compartments, CellLight
644 BacMam 2.0 reagents (Molecular Probes) for early endosomes (Rab5 red fluorescent protein
645 (RFP), Cat No. C10587) or lysosomes (LAMP1 RFP, Cat No. C10597) were added for 18 h prior to
646 addition of the tetramer. For all imaging, DAPI was added during PBS washes, and cells were fixed
647 prior to data acquisition. Images were acquired on a Keyence BZ-X810 Fluorescence microscope
648 or high-resolution wide-field CoreDV microscope (Applied Precision) with CoolSNAP ES2 HQ
649 (Nikon), using nuclear staining with DAPI to identify un-biased fields of view. Localization of the
650 tetramer to endosomal compartments was quantified using Imaris image analysis software [50].

651 *Data analysis, Statistics, and Reproducibility*

652 Data were analyzed with Prism 9 GraphPad Software. For measurements of functional avidity,
653 curves were determined by non-linear regression and best-fit EC_{50} was calculated. EC_{50} values
654 were compared with the extra sum-of-squares F test. Number of experimental and technical
655 replicates are specified in the figure legends.

656 Data Availability

657 The authors declare that the data supporting the findings of this study are available within the
658 paper and its supplementary information files. Plasmids are available via Addgene with the ID
659 numbers provided in the Methods section.

660 Acknowledgements

661 We would like to thank the participants who gave time and dedication to this health research as
662 well as Erin Merrifield, Department of Pediatrics, OHSU, for her contributions to this study.

This project has been funded in whole or in part with Federal funds from the National Institutes of Allergy and Infectious Diseases, National Institutes of Health, Department of Health and Human Services, under grant no AI147954 (EA, DML, WHH), AI134790 (DML), GM007183 (NAL), AI129976 (MH), R01AI141549-01A1 (FT) and AI165618 (AO). This work was also supported in part by Merit Award #I01 CX001562 from the U.S. Department of Veterans Affairs Clinical Sciences Research and Development Program (MJH), Merit Award #I01 BX000533 from the U.S. Department of Veterans Affairs Biomedical Laboratory (DML).

Author Contributions

CK, GS, NAL, DAL, EJA, DML and MH contributed to the conception and/or design of the work. CK and GS are joint first authors. DML and MH jointly supervised the work. MC, MN, DAL and DML contributed to clinical activities. AO, WHH, FT, EJA, DML and MH raised grants to fund the research. CK, GS, NAL, MC, MN, AW, CL, TA, JB, TNL, CMH, MEH, JK, LA, AO, WHH, SM, FT, DAL, EJA, DML and MH substantially contributed to the acquisition, analysis, or interpretation of data and drafting of the manuscript. All authors substantially contributed to revising and critically reviewing the manuscript for important intellectual content. All authors approved the final version of this manuscript to be published and agree to be accountable for all aspects of the work.

Competing Interests

The authors declare no competing interests.

References

1 Crowther, M. D. & Sewell, A. K. The burgeoning role of MR1-restricted T-cells in infection, cancer and autoimmune disease. *Curr Opin Immunol* **69**, 10-17, doi:10.1016/j.coi.2020.12.002 (2021).

2 Hinks, T. S. C. & Zhang, X. W. MAIT Cell Activation and Functions. *Front Immunol* **11**, 1014, doi:10.3389/fimmu.2020.01014 (2020).

3 Trowitzsch, S. & Tampé, R. Multifunctional Chaperone and Quality Control Complexes in Adaptive Immunity. *Annual Review of Biophysics* **49**, 135-161, doi:10.1146/annurev-biophys-121219-081643 (2020).

692 4 Alvaro-Benito, M. & Freund, C. Revisiting nonclassical HLA II functions in
693 antigen presentation: Peptide editing and its modulation. *HLA* **96**, 415-429,
694 doi:10.1111/tan.14007 (2020).
695 5 Moody, D. B. & Cotton, R. N. Four pathways of CD1 antigen presentation to T
696 cells. *Curr Opin Immunol* **46**, 127-133, doi:10.1016/j.coi.2017.07.013 (2017).
697 6 McWilliam, H. E. *et al.* The intracellular pathway for the presentation of
698 vitamin B-related antigens by the antigen-presenting molecule MR1. *Nat*
699 *Immunol* **17**, 531-537, doi:10.1038/ni.3416 (2016).
700 7 McWilliam, H. E. G. *et al.* Endoplasmic reticulum chaperones stabilize ligand-
701 receptive MR1 molecules for efficient presentation of metabolite antigens.
702 *Proc Natl Acad Sci U S A* **117**, 24974-24985, doi:10.1073/pnas.2011260117
703 (2020).
704 8 Corbett, A. J. *et al.* T-cell activation by transitory neo-antigens derived from
705 distinct microbial pathways. *Nature* **509**, 361-365, doi:10.1038/nature13160
706 (2014).
707 9 Harriff, M. J. *et al.* Endosomal MR1 Trafficking Plays a Key Role in Presentation
708 of Mycobacterium tuberculosis Ligands to MAIT Cells. *PLoS Pathog* **12**,
709 e1005524, doi:10.1371/journal.ppat.1005524 (2016).
710 10 Karamooz, E., Harriff, M. J., Narayanan, G. A., Worley, A. & Lewinsohn, D. M.
711 MR1 recycling and blockade of endosomal trafficking reveal distinguishable
712 antigen presentation pathways between Mycobacterium tuberculosis
713 infection and exogenously delivered antigens. *Scientific Reports* **9**, 4797,
714 doi:10.1038/s41598-019-41402-y (2019).
715 11 Kulicke, C., Karamooz, E., Lewinsohn, D. & Harriff, M. Covering All the Bases:
716 Complementary MR1 Antigen Presentation Pathways Sample Diverse
717 Antigens and Intracellular Compartments. *Frontiers in Immunology* **11**,
718 doi:10.3389/fimmu.2020.02034 (2020).
719 12 Lange, J. *et al.* The Chemical Synthesis, Stability, and Activity of MAIT Cell
720 Prodrug Agonists That Access MR1 in Recycling Endosomes. *ACS Chemical*
721 *Biology*, doi:10.1021/acschembio.9b00902 (2020).
722 13 Ussher, J. E. *et al.* TLR signaling in human antigen-presenting cells regulates
723 MR1-dependent activation of MAIT cells. *European Journal of Immunology* **46**,
724 1600-1614, doi:10.1002/eji.201545969 (2016).
725 14 McWilliam, H. E. G. & Salio, M. Understanding and modulating the MR1
726 metabolite antigen presentation pathway. *Molecular Immunology* **129**, 121-
727 126, doi:10.1016/j.molimm.2020.11.019 (2021).

728 15 Harriff, M. J. *et al.* MR1 displays the microbial metabolome driving selective
729 MR1-restricted T cell receptor usage. *Sci Immunol* **3**,
730 doi:10.1126/sciimmunol.aao2556 (2018).
731 16 Mak, J. Y. *et al.* Stabilizing short-lived Schiff base derivatives of 5-aminouracils
732 that activate mucosal-associated invariant T cells. *Nat Commun* **8**, 14599,
733 doi:10.1038/ncomms14599 (2017).
734 17 Priya, R. & Brutkiewicz, R. R. MR1 Tetramer-Based Artificial APCs Expand MAIT
735 Cells from Human Peripheral Blood That Effectively Kill Glioblastoma Cells.
736 *Immunohorizons* **5**, 500-511, doi:10.4049/immunohorizons.2100003 (2021).
737 18 Cruz, F. M., Chan, A. & Rock, K. L. Pathways of MHC I cross-presentation of
738 exogenous antigens. *Semin Immunol* **66**, 101729,
739 doi:10.1016/j.smim.2023.101729 (2023).
740 19 Gold, M. C. *et al.* Human mucosal associated invariant T cells detect bacterially
741 infected cells. *PLoS Biol* **8**, e1000407, doi:10.1371/journal.pbio.1000407
742 (2010).
743 20 Narayanan, G. A. *et al.* Alternative splicing of MR1 regulates antigen
744 presentation to MAIT cells. *Sci Rep* **10**, 15429, doi:10.1038/s41598-020-
745 72394-9 (2020).
746 21 Salio, M. *et al.* Ligand-dependent downregulation of MR1 cell surface
747 expression. *Proc Natl Acad Sci U S A* **117**, 10465-10475,
748 doi:10.1073/pnas.2003136117 (2020).
749 22 Lion, J. *et al.* MR1B, a natural spliced isoform of the MHC-related 1 protein, is
750 expressed as homodimers at the cell surface and activates MAIT cells. *Eur J*
751 *Immunol* **43**, 1363-1373, doi:10.1002/eji.201242461 (2013).
752 23 Salerno-Goncalves, R., Rezwan, T. & Sztein, M. B. B cells modulate mucosal
753 associated invariant T cell immune responses. *Front Immunol* **4**, 511,
754 doi:10.3389/fimmu.2013.00511 (2014).
755 24 Howson, L. J. *et al.* Absence of mucosal-associated invariant T cells in a person
756 with a homozygous point mutation in MR1. *Sci Immunol* **5**,
757 doi:10.1126/sciimmunol.abc9492 (2020).
758 25 Eckle, S. B. *et al.* A molecular basis underpinning the T cell receptor
759 heterogeneity of mucosal-associated invariant T cells. *J Exp Med* **211**, 1585-
760 1600, doi:10.1084/jem.20140484 (2014).
761 26 Lewinsohn, D. A. *et al.* Immunodominant tuberculosis CD8 antigens
762 preferentially restricted by HLA-B. *PLoS Pathog* **3**, 1240-1249,
763 doi:10.1371/journal.ppat.0030127 (2007).

764 27 Lancioni, C. *et al.* Recognition of CD8(+) T-cell epitopes to identify adults with
765 pulmonary tuberculosis. *Eur Respir J* **53**, doi:10.1183/13993003.02053-2018
766 (2019).
767 28 Adams, S. *et al.* HLA class I and II genotype of the NCI-60 cell lines. *J Transl*
768 *Med* **3**, 11, doi:10.1186/1479-5876-3-11 (2005).
769 29 Le Bourhis, L. *et al.* Antimicrobial activity of mucosal-associated invariant T
770 cells. *Nat Immunol* **11**, 701-708, doi:10.1038/ni.1890 (2010).
771 30 Bowman, E. J., Siebers, A. & Altendorf, K. Bafilomycins: a class of inhibitors of
772 membrane ATPases from microorganisms, animal cells, and plant cells. *Proc*
773 *Natl Acad Sci U S A* **85**, 7972-7976, doi:10.1073/pnas.85.21.7972 (1988).
774 31 Sadegh-Nasseri, S. Partnering for the major histocompatibility complex class
775 II and antigenic determinant requires flexibility and chaperons. *Curr Opin*
776 *Immunol* **70**, 112-121, doi:10.1016/j.coi.2021.05.005 (2021).
777 32 McShan, A. C. *et al.* TAPBPR employs a ligand-independent docking
778 mechanism to chaperone MR1 molecules. *Nat Chem Biol* **18**, 859-868,
779 doi:10.1038/s41589-022-01049-9 (2022).
780 33 Lim, H. J. *et al.* A specialized tyrosine-based endocytosis signal in MR1 controls
781 antigen presentation to MAIT cells. *J Cell Biol* **221**, doi:10.1083/jcb.202110125
782 (2022).
783 34 Scheller, R. H. In search of the molecular mechanism of intracellular
784 membrane fusion and neurotransmitter release. *Nat Med* **19**, 1232-1235,
785 doi:10.1038/nm.3339 (2013).
786 35 Spessott, W. A., Sanmillan, M. L., Kulkarni, V. V., McCormick, M. E. & Giraudo,
787 C. G. Syntaxin 4 mediates endosome recycling for lytic granule exocytosis in
788 cytotoxic T-lymphocytes. *Traffic* **18**, 442-452, doi:10.1111/tra.12490 (2017).
789 36 Kennedy, M. J., Davison, I. G., Robinson, C. G. & Ehlers, M. D. Syntaxin-4
790 defines a domain for activity-dependent exocytosis in dendritic spines. *Cell*
791 **141**, 524-535, doi:10.1016/j.cell.2010.02.042 (2010).
792 37 Chatterjee Bhowmick, D., Ahn, M., Oh, E., Veluthakal, R. & Thurmond, D. C.
793 Conventional and Unconventional Mechanisms by which Exocytosis Proteins
794 Oversee beta-cell Function and Protection. *Int J Mol Sci* **22**,
795 doi:10.3390/ijms22041833 (2021).
796 38 Black, H. L. *et al.* Knockout of syntaxin-4 in 3T3-L1 adipocytes reveals new
797 insight into GLUT4 trafficking and adiponectin secretion. *J Cell Sci* **135**,
798 doi:10.1242/jcs.258375 (2022).
799 39 Lamichhane, R. & Ussher, J. E. Expression and trafficking of MR1. *Immunology*
800 **151**, 270-279, doi:10.1111/imm.12744 (2017).

801 40 Karamooz, E., Harriff, M. J. & Lewinsohn, D. M. MR1-dependent antigen
802 presentation. *Seminars in Cell & Developmental Biology* **84**, 58-64,
803 doi:https://doi.org/10.1016/j.semcdb.2017.11.028 (2018).
804 41 Blander, J. M. Regulation of the Cell Biology of Antigen Cross-Presentation.
805 *Annu Rev Immunol* **36**, 717-753, doi:10.1146/annurev-immunol-041015-
806 055523 (2018).
807 42 Kinsella, R. L. *et al.* Perspectives and Advances in the Understanding of
808 Tuberculosis. *Annu Rev Pathol* **16**, 377-408, doi:10.1146/annurev-pathol-
809 042120-032916 (2021).
810 43 Ackerman, A. L., Kyritsis, C., Tampé, R. & Cresswell, P. Access of soluble
811 antigens to the endoplasmic reticulum can explain cross-presentation by
812 dendritic cells. *Nat Immunol* **6**, 107-113, doi:10.1038/ni1147 (2005).
813 44 Spooner, R. A., Smith, D. C., Easton, A. J., Roberts, L. M. & Lord, J. M.
814 Retrograde transport pathways utilised by viruses and protein toxins. *Virol J*
815 **3**, 26, doi:10.1186/1743-422x-3-26 (2006).
816 45 Mukhopadhyay, S. & Linstedt, A. D. Retrograde trafficking of AB_5 toxins:
817 mechanisms to therapeutics. *J Mol Med (Berl)* **91**, 1131-1141,
818 doi:10.1007/s00109-013-1048-7 (2013).
819 46 Hafstrand, I., Aflalo, A. & Boyle, L. H. Why TAPBPR? Implications of an
820 additional player in MHC class I peptide presentation. *Current Opinion in*
821 *Immunology* **70**, 90-94, doi:10.1016/j.coi.2021.04.011 (2021).
822 47 Thomas, C. & Tampe, R. MHC I assembly and peptide editing - chaperones,
823 clients, and molecular plasticity in immunity. *Curr Opin Immunol* **70**, 48-56,
824 doi:10.1016/j.coi.2021.02.004 (2021).
825 48 Kulicke, C. A. *et al.* The P5-type ATPase ATP13A1 modulates major
826 histocompatibility complex I-related protein 1 (MR1)-mediated antigen
827 presentation. *J Biol Chem* **298**, 101542, doi:10.1016/j.jbc.2021.101542
828 (2022).
829 49 Pankhurst, T. E. *et al.* MAIT cells activate dendritic cells to promote T(FH) cell
830 differentiation and induce humoral immunity. *Cell Rep* **42**, 112310,
831 doi:10.1016/j.celrep.2023.112310 (2023).
832 50 Harriff, M. J. *et al.* Human Lung Epithelial Cells Contain Mycobacterium
833 tuberculosis in a Late Endosomal Vacuole and Are Efficiently Recognized by
834 CD8+ T Cells. *PLOS ONE* **9**, e97515, doi:10.1371/journal.pone.0097515
835 (2014).

836 51 Jin, H. *et al.* Deaza-modification of MR1 ligands modulates recognition by
837 MR1-restricted T cells. *bioRxiv*, 2022.2005.2011.491531,
838 doi:10.1101/2022.05.11.491531 (2022).
839 52 Huber, M. E. *et al.* Rab6 regulates recycling and retrograde trafficking of MR1
840 molecules. *Sci Rep* **10**, 20778, doi:10.1038/s41598-020-77563-4 (2020).
841 53 Laugel, B. *et al.* Engineering of Isogenic Cells Deficient for MR1 with a
842 CRISPR/Cas9 Lentiviral System: Tools To Study Microbial Antigen Processing
843 and Presentation to Human MR1-Restricted T Cells. *J Immunol* **197**, 971-982,
844 doi:10.4049/jimmunol.1501402 (2016).
845 54 Olive, A. J. *et al.* Chlamydia trachomatis-induced alterations in the host cell
846 proteome are required for intracellular growth. *Cell Host Microbe* **15**, 113-
847 124, doi:10.1016/j.chom.2013.12.009 (2014).
848 55 Murhammer, D. W. e. *Baculovirus and insect cell expression protocols*. Vol.
849 388 (Humana Press, 2007).
850 56 Niekamp, P. *et al.* Sphingomyelin Biosynthesis Is Essential for Phagocytic
851 Signaling during Mycobacterium tuberculosis Host Cell Entry. *mBio* **12**,
852 doi:10.1128/mBio.03141-20 (2021).
853 57 Tafesse, F. G. *et al.* Disruption of Sphingolipid Biosynthesis Blocks
854 Phagocytosis of Candida albicans. *PLoS Pathog* **11**, e1005188,
855 doi:10.1371/journal.ppat.1005188 (2015).
856 58 Thomas, S. T., Wierenga, K. A., Pestka, J. J. & Olive, A. J. Fetal Liver-Derived
857 Alveolar-like Macrophages: A Self-Replicating Ex Vivo Model of Alveolar
858 Macrophages for Functional Genetic Studies. *Immunohorizons* **6**, 156-169,
859 doi:10.4049/immunohorizons.2200011 (2022).
860 59 Brinkman, E. K., Chen, T., Amendola, M. & van Steensel, B. Easy quantitative
861 assessment of genome editing by sequence trace decomposition. *Nucleic*
862 *Acids Res* **42**, e168, doi:10.1093/nar/gku936 (2014).
863 60 Conant, D. *et al.* Inference of CRISPR Edits from Sanger Trace Data. *Crispr j* **5**,
864 123-130, doi:10.1089/crispr.2021.0113 (2022).
865 61 Li, K. *et al.* Synthesis, stabilization, and characterization of the MR1 ligand
866 precursor 5-amino-6-D-ribitylaminouracil (5-A-RU). *PLoS One* **13**, e0191837,
867 doi:10.1371/journal.pone.0191837 (2018).
868 62 López-Sagaseta, J. *et al.* The molecular basis for Mucosal-Associated Invariant
869 T cell recognition of MR1 proteins. *Proc Natl Acad Sci U S A* **110**, E1771-1778,
870 doi:10.1073/pnas.1222678110 (2013).

871 63 Boulter, J. M. *et al.* Stable, soluble T-cell receptor molecules for crystallization
872 and therapeutics. *Protein Eng* **16**, 707-711, doi:10.1093/protein/gzg087
873 (2003).
874 64 Chang, H. C. *et al.* A general method for facilitating heterodimeric pairing
875 between two proteins: application to expression of alpha and beta T-cell
876 receptor extracellular segments. *Proc Natl Acad Sci U S A* **91**, 11408-11412,
877 doi:10.1073/pnas.91.24.11408 (1994).
878

879 Figure Legends

880 **Fig 1. MR1 ligands delivered to antigen presenting cells on soluble MR1 molecules are**
881 **efficiently recognized by MR1T cell clones. a.** MR1T cell clone (1e4) IFN-γ responses to MR1/5-
882 OP-RU or MR1/6-FP tetramer, either added to DCs (1e4) (exSPOT) or bound to ELISPOT plate
883 (tetraSPOT). **b.** MR1T cell clone (1e4) IFN-γ response to MR1/5-OP-RU is inhibited by anti-MR1
884 antibody blockade (aMR1, 2 µg/ml). **c**. MR1T cell clone (1e4) IFN-γ response to MR1/5-OP-RU
885 tetramer, added to either DCs, THP-1 cells, BEAS-2B (B2B) cells or B-LCL (1e4). EC_{50} calculated
886 using non-linear regression and the difference in the EC_{50} was statistically significant between
887 the curves ($p<0.0001$) by the extra sum-of-squares F test. Data are representative of n=3
888 independent experiments each. Technical duplicates within the representative experiment are
889 shown with a line connecting the mean. For EC_{50} values of replicate experiments see
890 Supplementary Tables 1+2.
891
892 **Fig 2. Ligand delivered in the context of MR1 monomer is presented more efficiently than free**
893 **ligand. a.** MR1T cell clone (1e4) IFN-γ response to DCs incubated with MR1/5-OP-RU tetramer,
894 MR1/5-OP-RU monomer, and soluble 5-OP-RU. EC_{50} calculated using non-linear regression. The
895 difference in the EC_{50} was statistically significant between the MR1/5-OP-RU tetramer and 5-OP-
896 RU and between MR1/5-OP-RU monomer and 5-OP-RU curves ($p<0.0001$), but there was no
897 significant difference in the EC_{50} of MR1/5-OP-RU tetramer and monomer by the extra sum-of-
898 squares F test ($p=0.7486$). Data are representative of n=3 independent experiments. Technical
899 duplicates within the representative experiment are shown with a line depicting the non-linear
900 regression curve. For EC_{50} values of replicate experiments see Supplementary Table 3. **b.** BEAS-
901 2B.MR1-GFP cells were incubated with the indicated concentrations of MR1/5-OP-RU monomer
902 or free 5-OP-RU overnight and surface stained for flow cytometry with APC-conjugated TCR
903 tetramer. Representative histograms are shown with pooled geometric mean fluorescence
904 intensity (GeoMFI) from n=4 experiments. The same unstained and untreated control are shown
905 in both histogram plots for easy comparison. Error bars denote SD of the mean of pooled
906 experiments which are shown individually in lighter colors.
907
908 **Fig 3. Presentation of MR1 ligands delivered on soluble MR1 molecules requires cellular MR1.**
909 **a.** MR1T cell clone (1e3) IFN-γ response to BEAS-2B, BEAS-2B *MR1*$^{-/-}$ and BEAS-2B *MR1*$^{-/-}$: *MR1A*
910 (1e4) incubated with MR1/5-OP-RU or MR1/6-FP monomers. Also included MR1T clone IFN-γ
911 response to MR1/5-OP-RU monomer only with no antigen presenting cells. **b.** Same as **a.**, except
912 the antigen presenting cells are THP-1, THP-1 *MR1*$^{-/-}$ and THP-1 *MR1*$^{-/-}$: *MR1A* (1e4). Data are
913 representative of n=2 independent experiments. Technical duplicates within the representative
914 experiment are shown with a line connecting the mean.
915
916 **Fig 4. Ligands are transferred from the soluble MR1 molecules onto cellular MR1.**
917 **a.** BEAS-2B.MR1-GFP cells (3e5) were pre-incubated with 50 nM of MR1/5-OP-RU monomer
918 overnight before staining with either Streptavidin (i), TCR tetramer (ii) or biotinylated 26.5 anti-
919 MR1 antibody followed by Streptavidin (iii). The same unstained sample is shown in all panels
920 and the same primary antibody only controls are shown in (i) and (iii) for easy comparison. Data

921 are representative of n=3 independent experiments. **b.** BEAS-2B.MR1-GFP cells were pre-
922 incubated with 10 μM of latrunculin B (LatB) for 1 h before addition of MR1/5-OP-RU or MR1/6-
923 FP monomer for an additional 4 h. Cells were surface stained with TCR tetramer. Representative
924 histograms are shown with pooled geometric mean fluorescence intensity (GeoMFI) from n=3
925 experiments. The same unstained and untreated control are shown in both histogram plots for
926 easy comparison. Error bars denote SD. Bar denotes mean. **c**. BEAS-2B.MR1-GFP cells were
927 incubated with either 50 nM MR1/5-OP-RU monomer or 6.4 μM of free 5-OP-RU for indicated
928 amounts of time before surface staining for flow cytometry with TCR tetramer. Representative
929 histograms are shown with pooled geometric mean fluorescence intensity (GeoMFI) from n=3
930 experiments. Error bars denote SD of the mean of pooled experiments which are shown
931 individually in lighter colors. **d.** MR1T cell clone (1e3) IFN-γ response to BEAS-2B *MR1*$^{-/-}$ cells (1e4)
932 that had been transfected with the pCI AscI MR1 res or pCI AscI MR1 R9H res plasmid, followed
933 by addition of the MR1/5-OP-RU monomer, or 1 μL of *M. smegmatis* supernatant. Data are
934 representative of n=3 independent experiments. Technical duplicates within the representative
935 experiment are shown with a line connecting the mean.
936
937 **Fig 5. Ligand exchange can occur in post-ER compartments. a.** MR1T cell clone (1e4) IFN-γ
938 response to BEAS-2B.MR1-GFP (1e4) that were pretreated with 6-FP *vs* NaOH using MR1/5-OP-
939 RU monomer as the antigen. EC_{50} calculated using non-linear regression and the difference in the
940 EC_{50} was statistically significant between the curves ($p<0.0001$) by the extra sum-of-squares F
941 test. For EC_{50} values of replicate experiments see Supplementary Table 4. **b.** HLA*B08:01-
942 restricted T cell clone D480-F6 was stained with the HLA-B*08:01 tetramer to $CFP10_{3-11}$, along
943 with antibodies to CD3, CD4, CD8 and a live/dead discriminator. Live, $CD3^+CD4^-CD8^+$ T cells are
944 shown. **c.** HLA*B08:01-restricted T cell clone D480-F6 (5e3) IFN-γ response to DCs (1e4) that were
945 incubated with either the $CFP10_{3-11}$ tetramer or $CFP10_{3-11}$ peptide. 9.5e4 irrelevant T cells (MR1-
946 restricted D426-G11) were also added to the well to decrease T:T presentation of the classical T
947 cell clone. **d.** MHC II-restricted T cell clone D481-D1 was stained with the HLA-DRB1*14:03
948 tetramer to $Esat6_{73-87}$ or a control tetramer along with antibodies to CD3, CD4, CD8 and a
949 live/dead discriminator. Live, $CD3^+CD8^-CD4^+$ T cells are shown. **e.** MHC II-restricted T cell clone
950 D481-D1 (2e4) IFN-γ response to D481 (autologous) dendritic cells (2e4) that were incubated with
951 either the $Esat6_{73-87}$ tetramer, control tetramer or $Esat6_{73-87}$ peptide. **f.** MHC II-restricted D481-
952 D1 T cell clone (2e4) IFN-γ response to D481 (autologous) DCs, D520 mismatched dendritic cells
953 or A549 cells (2e4) that were incubated with the $Esat6_{73-87}$ tetramer. **g.** BEAS-2B.MR1-GFP cells
954 were pre-incubated with 6-FP or NaOH overnight. 6-FP was washed off and cells were incubated
955 with 50 ug/ml brefeldin A (BFA) for 1h before addition of MR1/5-OP-RU or MR1/6-FP monomer
956 for an additional 4 h. Cells were surface stained for flow cytometry with TCR tetramer.
957 Representative histograms are shown with pooled geometric mean fluorescence intensity
958 (GeoMFI) from n=3 experiments. The same unstained control is shown in all plots. Error bars
959 denote SD. Bars denote mean. Data in **a**, **c**, **e** and **f** are representative of n=3 independent
960 experiments. In **a** and **c**, technical duplicates within the representative experiment are shown
961 with a line connecting the mean. In **e** and **f**, technical duplicates witin the representative
962 experiment are shown with the bar showing the mean.
963

964 **Fig. 6. Ligand exchange does not require acidification.**
965 **a.** BEAS-2B cells (1e5 or 1e4) were seeded on chamber slides and CellLight RFP reagents for Rab5
966 and LAMP1 were added and incubated for 18 h at 37C. Tetramer was then added for 2 h at room
967 temperature, followed by washing 2X in PBS. All images acquired were using the same
968 microscope settings. Data are representative of n=3 independent experiments. Error bars denote
969 SD of n=19 cells for Rab5 and n=17 cells for LAMP1 from a representative experiment. Scale bar
970 denotes 20 µm. **b.** MR1T cell clone (5e3) IFN-γ response to BEAS-2B (1e4) pre-treated with
971 Bafilomycin A1 for 2 h, followed by addition of the MR1/5-OP-RU monomer or 5-OP-RU prodrug.
972 Data are representative of n=3 independent experiments. Technical duplicates within the
973 representative experiment are shown with a line connecting the mean. **c**. MR1T cell clone (1e3)
974 IFN-γ response to BEAS-2B.Cas9 or BEAS-2B.Cas9 *STX4* KO cells (1e4) in the presence of the
975 indicated concentrations of *M. smegmatis* supernatant or MR1/5-OP-RU monomer. Data were
976 normalized to the maximum response and pooled from n=3 independent experiments. Error bars
977 denote SD of the mean of pooled experiments which are shown individually in lighter colors. EC_{50}
978 calculated using non-linear regression and the difference in the EC_{50} was statistically significant
979 between the curves (p=0.0032) by the extra sum-of-squares F test.

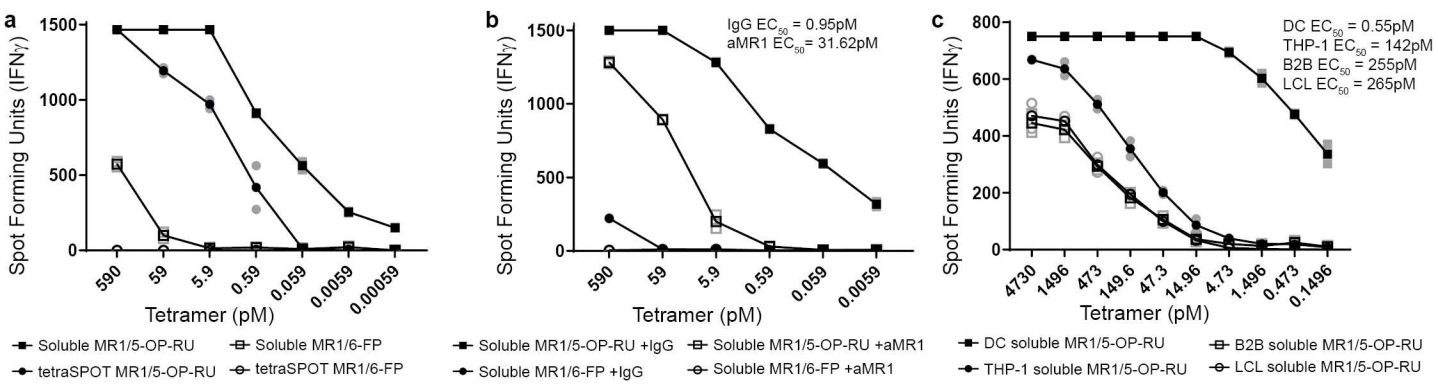
a
Spot Forming Units (IFNγ)
1500
1000
500
0
590
59
5.9
0.59
0.059
0.0059
0.00059
Tetramer (pM)
Soluble MR1/5-OP-RU
Soluble MR1/6-FP
tetraSPOT MR1/5-OP-RU
tetraSPOT MR1/6-FP
b
IgG EC50 = 0.95pM
aMR1 EC50 = 31.62pM
Spot Forming Units (IFNγ)
1500
1000
500
0
590
59
5.9
0.59
0.059
0.0059
Tetramer (pM)
Soluble MR1/5-OP-RU +IgG
Soluble MR1/5-OP-RU +aMR1
Soluble MR1/6-FP +IgG
Soluble MR1/6-FP +aMR1
c
DC EC50 = 0.55pM
THP-1 EC50 = 142pM
B2B EC50 = 255pM
LCL EC50 = 265pM
Spot Forming Units (IFNγ)
800
600
400
200
0
4730
1496
473
149.6
47.3
14.96
4.73
1.496
0.473
0.1496
Tetramer (pM)
DC soluble MR1/5-OP-RU
B2B soluble MR1/5-OP-RU
THP-1 soluble MR1/5-OP-RU
LCL soluble MR1/5-OP-RU

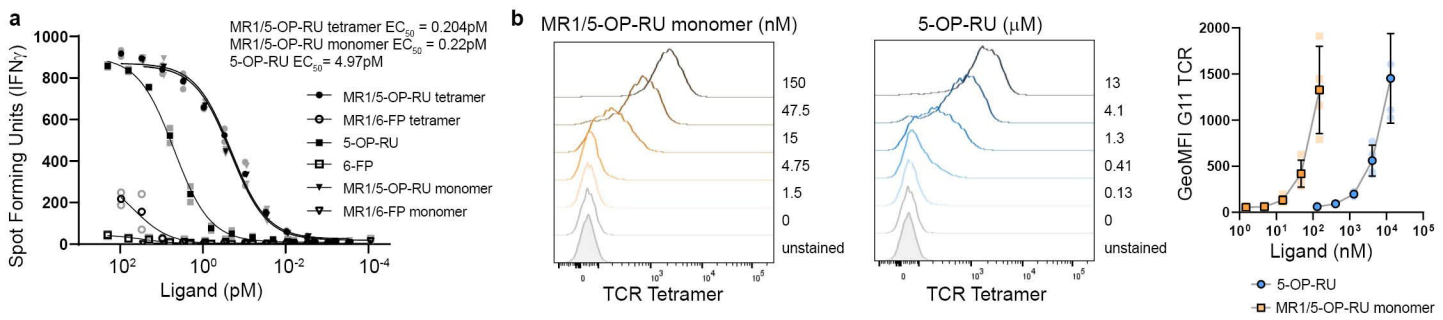
a
MR1/5-OP-RU tetramer EC50 = 0.204pM
MR1/5-OP-RU monomer EC50 = 0.22pM
5-OP-RU EC50 = 4.97pM
MR1/5-OP-RU tetramer
MR1/6-FP tetramer
5-OP-RU
6-FP
MR1/5-OP-RU monomer
MR1/6-FP monomer
Spot Forming Units (IFNγ)
Ligand (pM)
b
MR1/5-OP-RU monomer (nM)
150
47.5
15
4.75
1.5
0
unstained
TCR Tetramer
5-OP-RU (μM)
13
4.1
1.3
0.41
0.13
0
unstained
TCR Tetramer
GeoMFI G11 TCR
Ligand (nM)
5-OP-RU
MR1/5-OP-RU monomer

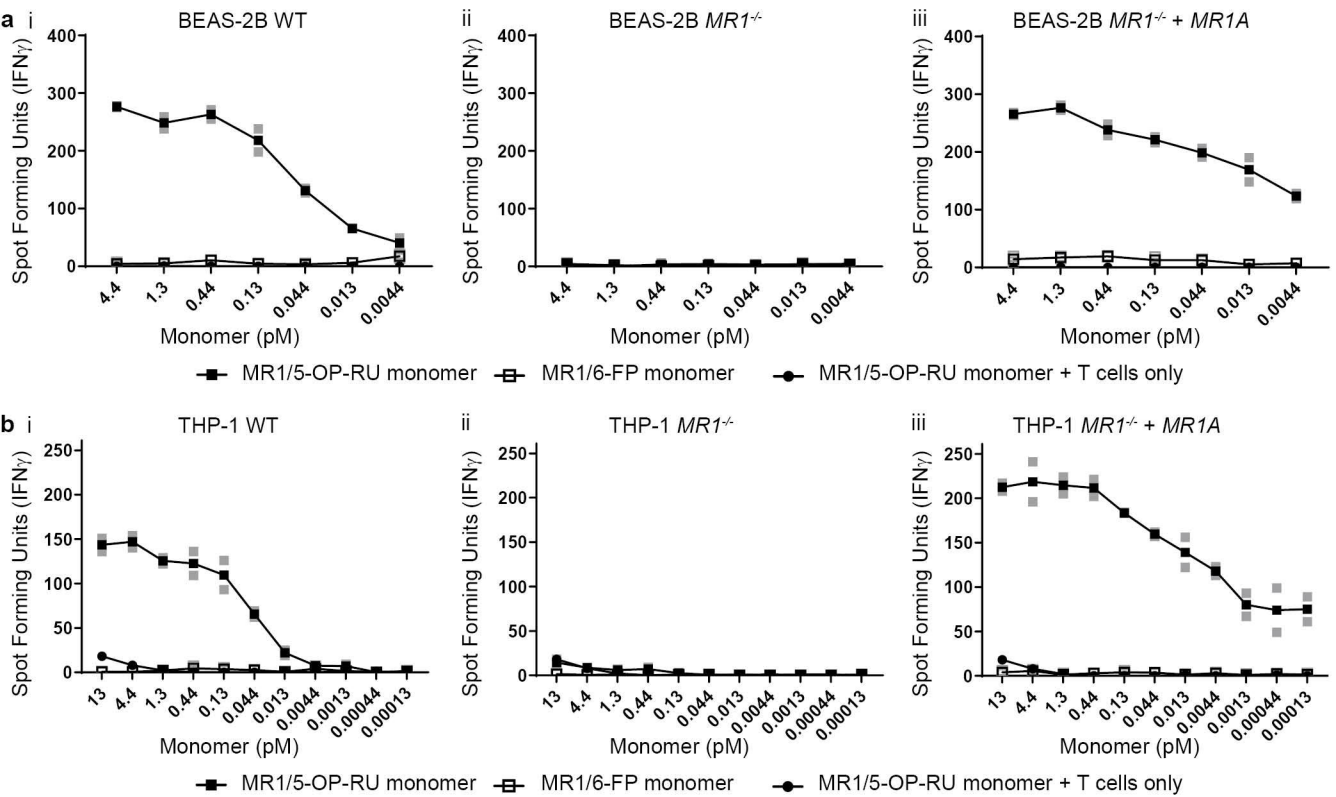
a
i
BEAS-2B WT
ii
BEAS-2B MR1-/-
iii
BEAS-2B MR1-/- + MR1A
Spot Forming Units (IFNγ)
400
300
200
100
0
4.4
1.3
0.44
0.13
0.044
0.013
0.0044
Monomer (pM)
MR1/5-OP-RU monomer
MR1/6-FP monomer
MR1/5-OP-RU monomer + T cells only
b
i
THP-1 WT
ii
THP-1 MR1-/-
iii
THP-1 MR1-/- + MR1A
Spot Forming Units (IFNγ)
250
200
150
100
50
0
13
4.4
1.3
0.44
0.13
0.044
0.013
0.0044
0.0013
0.00044
0.00013
Monomer (pM)
MR1/5-OP-RU monomer
MR1/6-FP monomer
MR1/5-OP-RU monomer + T cells only

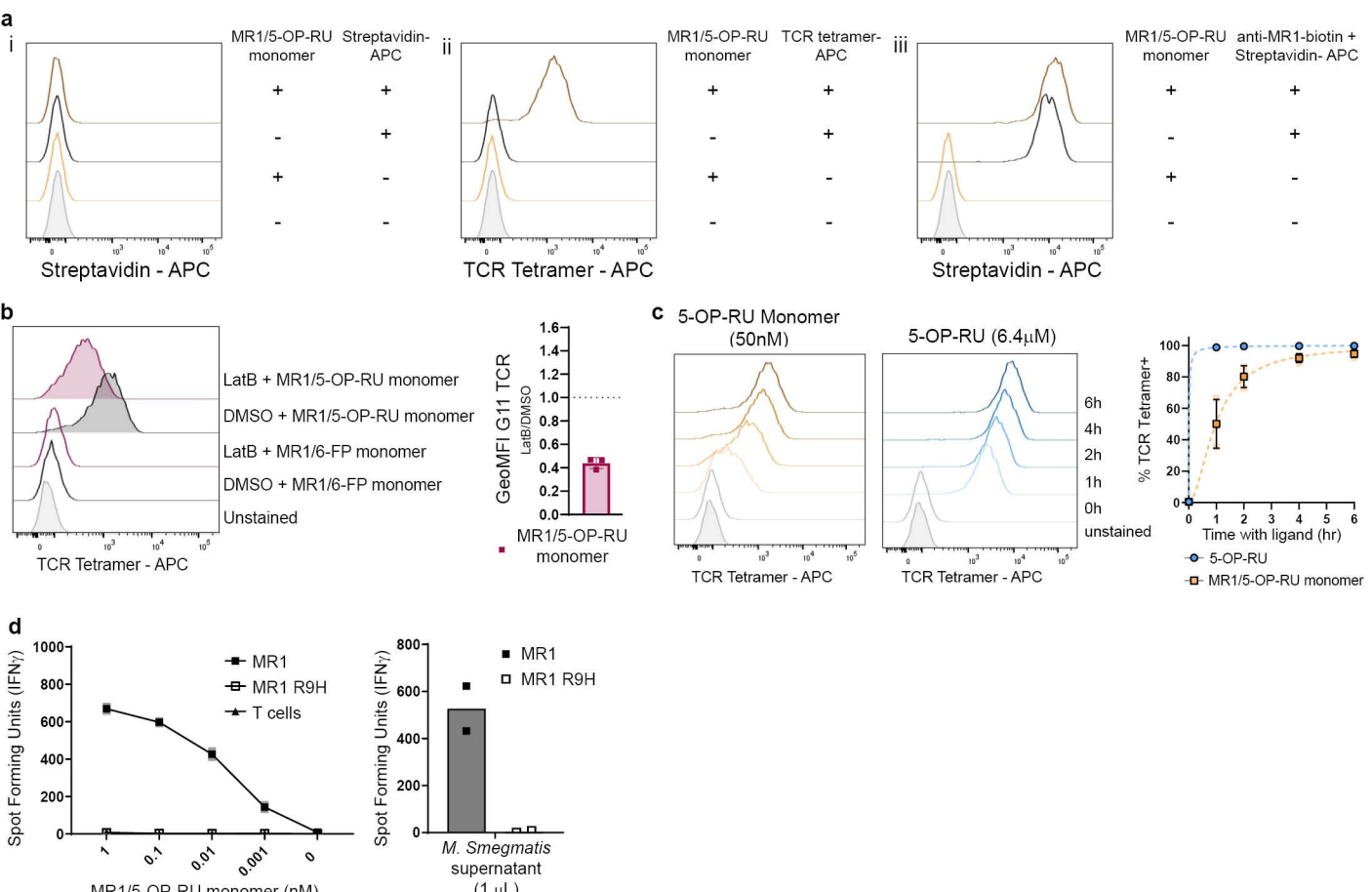
a
i
MR1/5-OP-RU monomer
Streptavidin-APC
Streptavidin - APC
ii
MR1/5-OP-RU monomer
TCR tetramer-APC
TCR Tetramer - APC
iii
MR1/5-OP-RU monomer
anti-MR1-biotin + Streptavidin- APC
Streptavidin - APC
b
LatB + MR1/5-OP-RU monomer
DMSO + MR1/5-OP-RU monomer
LatB + MR1/6-FP monomer
DMSO + MR1/6-FP monomer
Unstained
TCR Tetramer - APC
GeoMFI G11 TCR
LatB/DMSO
MR1/5-OP-RU monomer
c
5-OP-RU Monomer (50nM)
5-OP-RU (6.4μM)
6h
4h
2h
1h
0h
unstained
TCR Tetramer - APC
% TCR Tetramer+
Time with ligand (hr)
5-OP-RU
MR1/5-OP-RU monomer
d
MR1
MR1 R9H
T cells
Spot Forming Units (IFNγ)
MR1/5-OP-RU monomer (nM)
M. Smegmatis supernatant (1 μL)

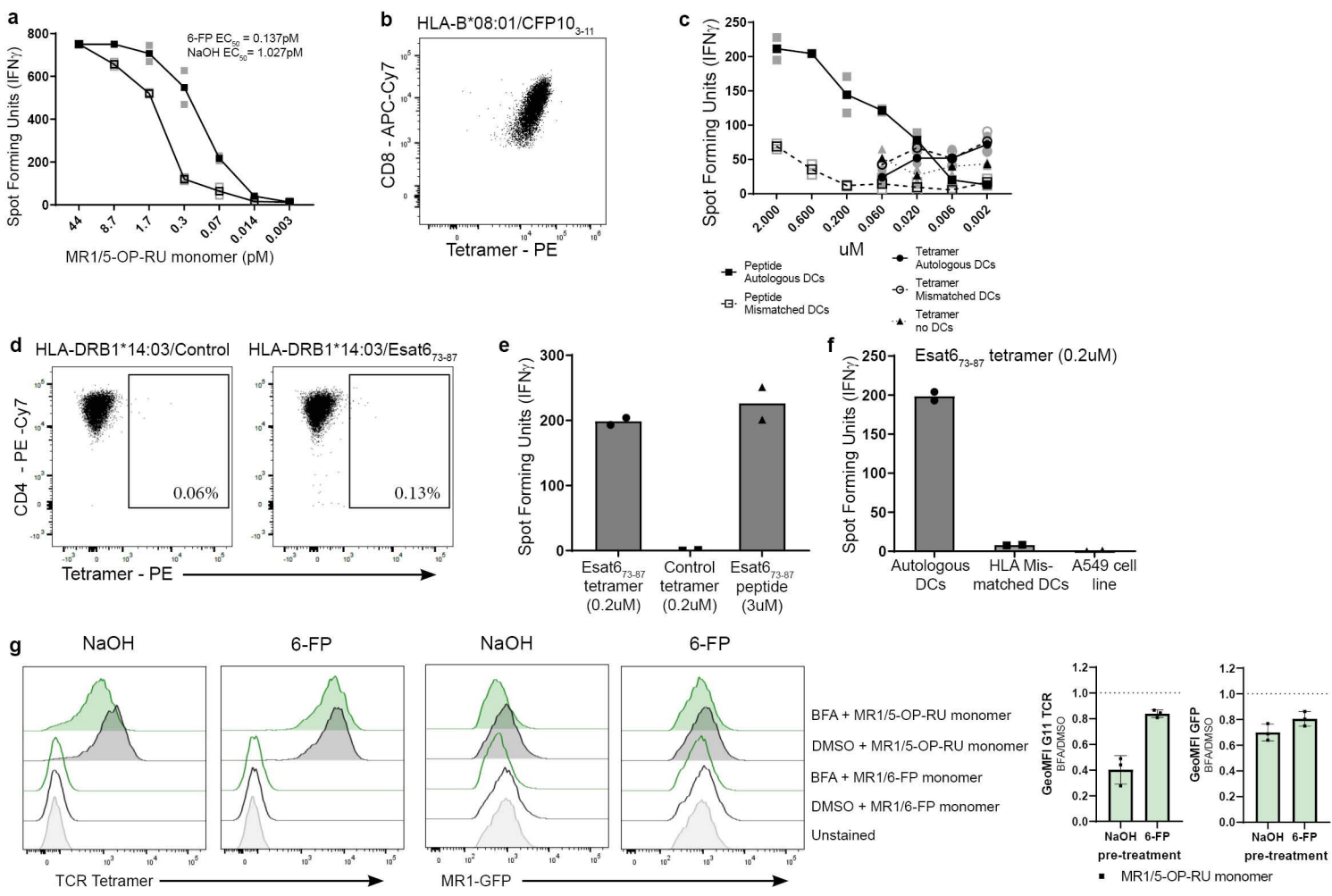
a
6-FP EC50 = 0.137pM
NaOH EC50 = 1.027pM
Spot Forming Units (IFNγ)
MR1/5-OP-RU monomer (pM)
b
HLA-B*08:01/CFP10 3-11
CD8 - APC-Cy7
Tetramer - PE
c
Spot Forming Units (IFNγ)
uM
Peptide Autologous DCs
Peptide Mismatched DCs
Tetramer Autologous DCs
Tetramer Mismatched DCs
Tetramer no DCs
d
HLA-DRB1*14:03/Control
HLA-DRB1*14:03/Esat6 73-87
CD4 - PE -Cy7
0.06%
0.13%
Tetramer - PE
e
Spot Forming Units (IFNγ)
Esat6 73-87 tetramer (0.2uM)
Control tetramer (0.2uM)
Esat6 73-87 peptide (3uM)
f
Esat6 73-87 tetramer (0.2uM)
Spot Forming Units (IFNγ)
Autologous DCs
HLA Mis-matched DCs
A549 cell line
g
NaOH
6-FP
NaOH
6-FP
BFA + MR1/5-OP-RU monomer
DMSO + MR1/5-OP-RU monomer
BFA + MR1/6-FP monomer
DMSO + MR1/6-FP monomer
Unstained
TCR Tetramer
MR1-GFP
GeoMFI G11 TCR BFA/DMSO
GeoMFI GFP BFA/DMSO
NaOH
6-FP
pre-treatment
MR1/5-OP-RU monomer

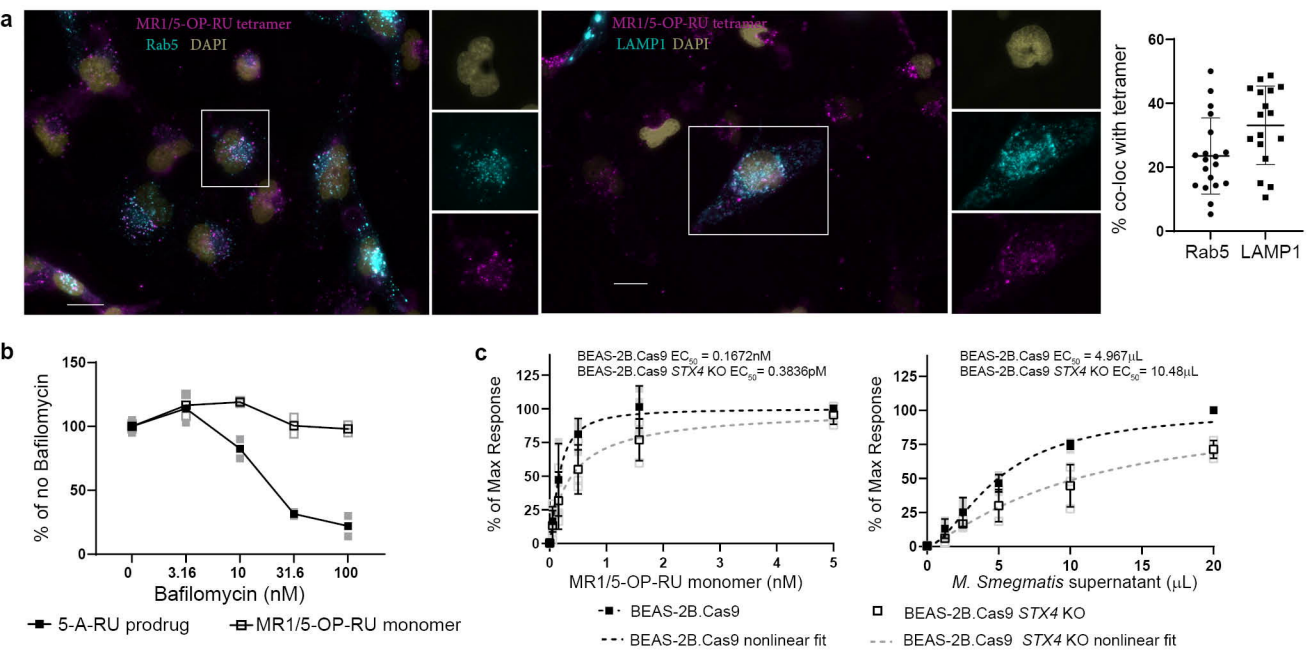
a
MR1/5-OP-RU tetramer
Rab5 DAPI
MR1/5-OP-RU tetramer
LAMP1 DAPI
% co-loc with tetramer
Rab5
LAMP1
b
% of no Bafilomycin
Bafilomycin (nM)
5-A-RU prodrug
MR1/5-OP-RU monomer
c
BEAS-2B.Cas9 EC50 = 0.1672nM
BEAS-2B.Cas9 STX4 KO EC50 = 0.3836pM
% of Max Response
MR1/5-OP-RU monomer (nM)
BEAS-2B.Cas9
BEAS-2B.Cas9 nonlinear fit
BEAS-2B.Cas9 EC50 = 4.967µL
BEAS-2B.Cas9 STX4 KO EC50 = 10.48µL
M. Smegmatis supernatant (µL)
BEAS-2B.Cas9 STX4 KO
BEAS-2B.Cas9 STX4 KO nonlinear fit